



Research Article

Palaeosedimentary Environment and Formation Mechanism of High-Quality Xujiache Source Rocks, Sichuan Basin, South China

Kun Xu ¹, Shijia Chen ^{1,2,3}, Jungang Lu,^{1,2,3} Yong Li,^{1,2,3} Xingcheng Zhu,¹ Jihua Liu,⁴ Xueting Wu,¹ and Chen Li¹

¹School of Geoscience and Technology, Southwest Petroleum University, Chengdu 610500, China

²Key Laboratory of Natural Gas Geology, Southwest Petroleum University, Chengdu 610500, China

³State Key Laboratory of Reservoir Geology and Development Engineering, Southwest Petroleum University, Chengdu, Sichuan 610500, China

⁴Dongxin Oil Production Plant, Shengli Oilfield Branch, Sinopec, Dongying, Shandong 257000, China

Correspondence should be addressed to Shijia Chen; 939543599@qq.com

Received 24 March 2022; Accepted 16 July 2022; Published 29 July 2022

Academic Editor: Xiangyang Xie

Copyright © 2022 Kun Xu et al. Exclusive Licensee GeoScienceWorld. Distributed under a Creative Commons Attribution License (CC BY 4.0).

Triassic Xujiache source rocks, the main gas source of shallow tight gas, are the most typical continental coal-bearing source rocks in the Sichuan Basin, South China. However, the organic matter enrichment section cannot be identified easily, leading to limited progress in the exploration of coal-bearing tight gas. This paper reveals the main controlling factors of the organic matter enrichment, reconstructs the evolution process of the Xujiache palaeosedimentary environment, proposes a dynamic enrichment mechanism of the organic matter, and determines the organic matter enrichment section of the high-quality coal-bearing source rocks by geochemical characteristics of the source rocks, major elements, and trace elements. The results show that the Xujiache sedimentary environment can be divided into a fluctuating stage of transitional sedimentation, stable stage of transitional sedimentation, fluctuating stage of continental sedimentation, and stable stage of continental sedimentation. The Xujiache source rocks were featured with high-quality coal-bearing source rocks with high total organic carbon and maturity and good parent material in the stable stage of transitional sedimentation and fluctuating stage of continental sedimentation, in which the water was connected with the Palaeo-Tethys Ocean with abundant terrestrial organisms. The water was shallow in the fluctuating stage of transitional sedimentation with a low sedimentation rate, leading to poor organic matter enrichment. The Palaeo-Tethys Ocean withdrew westward from the Yangtze plate in the late period of the fluctuating stage of continental sedimentation, leading to the absence of algae and dinosteranes and a decrease in biological productivity in the stable stage of continental sedimentation. Therefore, high terrestrial inputs and biological productivity and high sedimentation rate were conducive to the organic matter preservation in the coal-bearing source rocks.

1. Introduction

The Xujiache source rocks are the most typical continental coal-bearing source rocks in South China with high organic matter abundance and large sedimentary thickness. It is considered the largest potential development target of the continental coal-bearing tight gas in the Sichuan Basin [1, 2]. Xujiache natural gas resources reached 2.41 trillion cubic feet. The restoration of the palaeoenvironment and organic matter evolution in the Xujiache source rocks are vital for analyzing the palaeoenvironmental evolution and the formation of

the high-quality coal-bearing source rocks. However, the dominant organic matter enrichment factors hinder the progress of continental coal-bearing tight gas exploration in the continental source rocks.

Initially, the global climate was considered to be warm and humid during the Triassic period [3, 4]. Subsequently, the distinct global climate was identified in the Triassic period with the further study of different regions. For example, Tian et al. [5] found that a cold climate period exists in the Triassic based on a new fossil wood species. Tanner et al. [6] analyzed the carbon isotope of calcite in soil and

suggested that the carbon dioxide and climate temperature increase at the end of the Triassic. Hochuli and Vigran [7] analyzed palynological records and found that the South Pole is ice-free. Moreover, anoxic events have been widely discussed at the end of the Triassic [8–12].

The closure of the Palaeo-Tethys Ocean (PTC) was also an important global event at the end of the Triassic [13–15]. The specific time of the PTC withdrawal of the Xujiahe sedimentary period affected the space-time pattern of the Eastern PTC and the reconstruction of the Pangaea in Southeast Asia [16, 17]. Previous studies on the PTC closure from the Yangtze plate were mainly characterized by sedimentary characteristics, tectonic deformation, and paleontological flora in the Xujiahe sedimentary period [18–20]. However, these studies do not give a specific time when the PTC ocean completely withdrew from the Xujiahe water in the Yangtze plate.

Furthermore, the main controlling factors of organic matter enrichment were debatable because of the distinct sedimentary environments in different regions. For example, Xiao et al. [21] and Yan et al. [22] reported that organic matter enrichment is controlled by water redox conditions. Nie et al. [23] proposed that palaeoclimatic conditions control organic matter enrichment. Wakefield [24] argued that organic matter enrichment is controlled by biological productivity. Mohialdeen and Hakimi [25] believed that organic matter enrichment is mainly controlled by palaeoproductivity and water salinity. Li et al. [26] suggested that organic matter enrichment is mainly influenced by terrestrial inputs or high productivity. However, current research focuses on the marine source rocks. Moreover, the environment is more complex in the continental or transitional facies comparable with the ocean sedimentary environment, leading to a more uncertain mechanism of organic matter enrichment.

This work studies the main controlling factors of the organic matter enrichment, reconstructs the palaeoenvironmental evolution of the Xujiahe period in the Sichuan Basin, and proposes the dynamic mechanism of the high-quality coal-bearing organic matter enrichment by organic and inorganic geochemical methods. The results further reveal the time of the PTC withdrawal from the Xujiahe sedimentation and its impact on the coal-bearing organic matter enrichment in the lake basin. This study has vital reference value for the spatial and temporal evolution pattern of the PTC, and the exploration and development of the coal-bearing natural gas in the Sichuan Basin and similar basins.

2. Geological Setting

The Sichuan Basin is a large intracratonic basin in southwest China that formed after the uplift of the Yangtze plate owing to the collision between the Indian and Eurasian plates [27]. The Sichuan Basin was initially surrounded by mountains at the end of the Triassic [28]. Furthermore, the northern margin of the Yangtze block was always a passive continental margin during the Late Paleozoic, characterized by the development of shallow sea shelves, slope clastic, and carbonate deposits [28]. The Yangtze block collided with the outer block in the Middle to Late Triassic, and the Mianlue

suture eventually joined North China and the Yangtze block. The Mianlue suture (the boundary between the Yangtze plate and the Qinling-Dabie Mountains) was formed by the PTC closure from east to west [29]. The flysch was also developed in the Diebu-Songpan area in the north of the Yangtze plate as the Yangtze plate moved northwest and subducted diagonally under the Qinling-Dabie Mountains. Moreover, the continental molasse was also first formed in the northern Yangtze plate in response to the initial collision. The Triassic sediments entered the continental sedimentary stage because the Palaeo-Tethys Ocean also withdrew from the Yangtze plate from west to east at the end of the Late Triassic [30]. The Longmenshan tectonic belt was also formed in the Late Triassic [31]. Additionally, the Sichuan Basin is the largest natural gas-producing area in China, and the Xujiahe source rocks are the only coal-bearing source rocks [29, 32, 33]. The study area is located in the middle of the Sichuan Basin and is tectonically located in the uplift belt of the Centre Sichuan, sandwiched between Chengdu and Chongqing (Figure 1). The widely discovered coal-bearing tight gas fields are mostly distributed in this area [27, 34].

Upper Triassic Formations include the Maantang, Xiaotangzi, and Xujiahe Formations (Figure 1). The Xujiahe Formation is divided into the second, third, fourth, fifth, and sixth members (henceforth referred to as Mb. 2, Mb. 3, Mb. 4, Mb. 5, and Mb. 6, respectively). Noting that in China, the Xiaotangzi Formation is equal to the first member of the Xujiahe Formation (Mb. 1). The Maantang and Xiaotangzi Formations are mainly featured by limestones and mudstones, and sandstones and mudstones, respectively [35]. The 2nd, 4th, and 6th Mbs. are mainly developed in sandstones. In contrast, the 1st, 3rd, and 5th Mbs. are mainly characterized by mudstones. Biohillocks, oolitic shoals, and mudstones were mainly developed in the Maantang sedimentary period [36]. The terrigenous debris increased with the expansion of the sea area during the period of the Mb. 1 in which mudstones and sandstones were developed [32, 36]. The Mb. 3 was characterized by transitional sediments [37]. The sedimentary centre was not consistent with the sedimentary-subsidence centre. The sedimentary-subsidence centre was located in the Wushan-Longfengchang area in the Western Sichuan; the sedimentary centre was located in the Bajiaochang-Jinhua area of the Centre Sichuan, where the calcite rocks (limestone or marl) were relatively developed with the relatively deep water depth [38]. The area connected with the seawater might also develop in the vicinity of the Anxian and Beichuan, where limestones were developed [38, 39]. The Mb. 5 was mainly characterized by continental deposits owing to the uplift of the Longmenshan belt. The surrounding mountains were also relatively quiet in the 3rd Mb. sedimentary period [32, 40]. Briefly, mudstones are developed in the Mb. 1, Mb. 3, and Mb. 5 because the source supply rate is less than the basin subsidence rate. Sandstones are developed in the Mb. 2, Mb. 4, and Mb. 6 because the source supply rate is higher than the basin subsidence rate [37, 41]. Moreover, the source rocks are mainly developed in the Mb. 3 and Mb. 5 in the study area. The mudstones are thinned in the Mb. 1 in the Centre Sichuan, whereas the

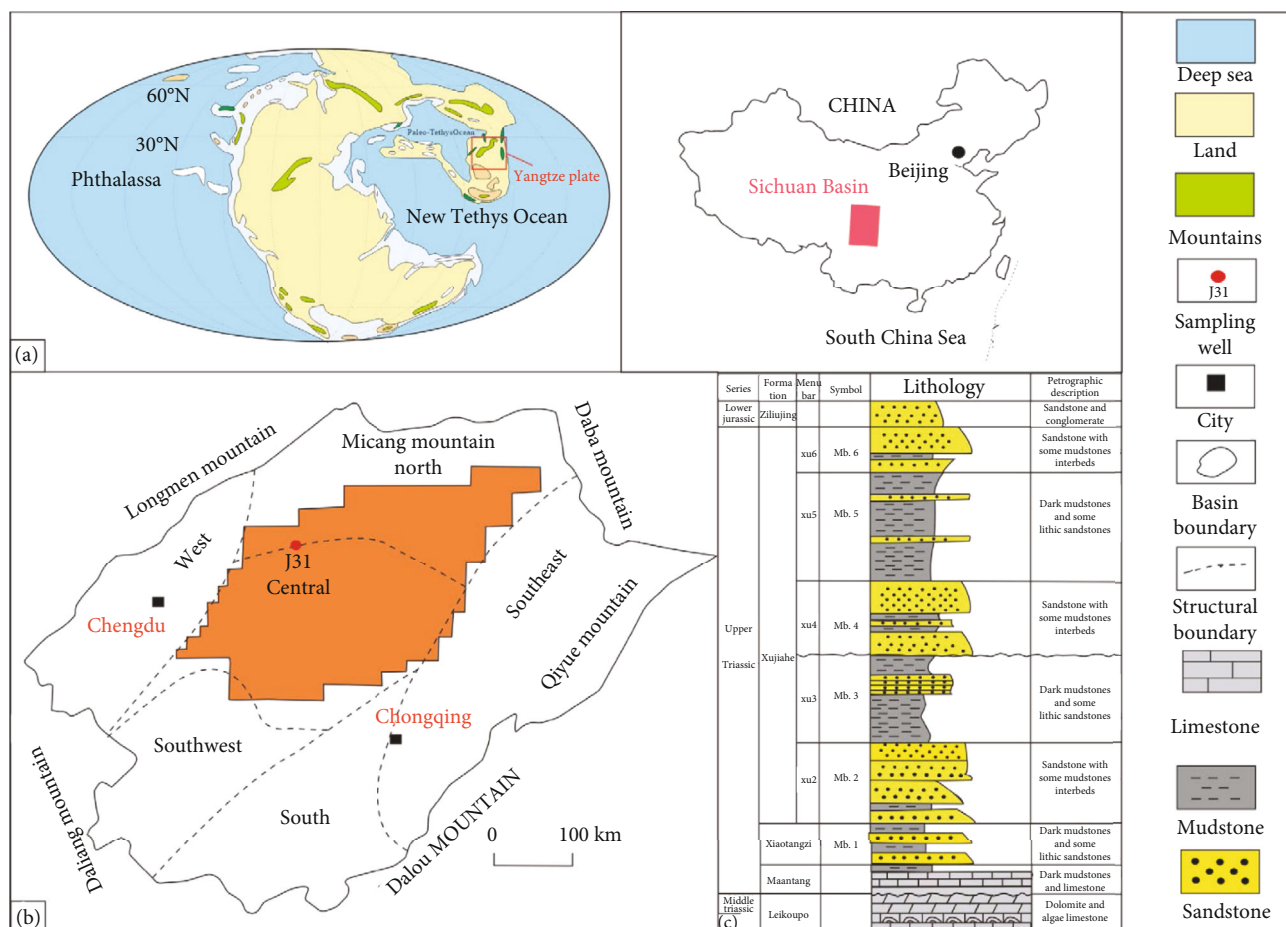


FIGURE 1: Location and lithology column of the study area. (a) Global Palaeogeographic World Map of the Late Triassic, modified from Golonka et al. [82]. (b) Location of the study area and outline of the Sichuan Basin. (c) Stratigraphic structure and lithology of Xujiache Formation in the Sichuan Basin. The orange area represents the central part of Sichuan in the study of the oil-gas fields.

sandstones develop. The thick sand bodies of the study area are widely developed in the Mb. 2, Mb. 4, and Mb. 6 (Figure 1).

3. Samples and Experimental Methods

3.1. Samples. Twenty-eight source rock samples were selected from the core of well J31 in the Centre Sichuan for organic geochemical characteristics according to the characteristics of various lithologies (Tables 1 and 2). Twenty-eight samples were selected to test trace and major elements (Tables 3 and 4), 6 samples from the Mb. 3, 17 samples from the Mb. 5, and 3 samples from the Mb. 1. The 1st Mb. mudstone debris was only obtained without collecting the core owing to the low development degree of the 1st Mb. mudstone in the Centre Sichuan. Two sandy mudstones were also selected from the Mb. 4.

3.2. Geochemical Analysis of Source Rocks. The total organic carbon (TOC) and kerogen maceral tests were conducted at the State Key Laboratory of Oil and Gas Reservoir Geology and Development Engineering, Southwest Petroleum University. The test instrument for TOC was a Leco CS-200 car-

bon and sulfur detector. The samples were first ground to particle sizes less than 0.2 mm, and the inorganic carbon in the samples was then removed with dilute hydrochloric acid. Finally, the TOC was converted to carbon dioxide by combustion using high-temperature oxygen flow. The TOC content was calculated using an infrared detector. Specific operation methods can be referred to as the Chinese national standard GB/T 19145-2003.

Initially, 50 g of the mudstone sample was taken as pulverized powder in the determination of kerogen macerals. The hydrofluoric acid and hydrochloric acid were then used for repeated dissolution, and the kerogen was separated by centrifugation and dried subsequently. The prepared kerogen sample was coated on a glass sheet to form a thin sheet. The macerals in the kerogen were observed, identified, and counted under a microscope. The type index (TI) of kerogen samples was obtained using different weighting coefficients for different macerals, and the kerogen samples were divided into types I, II₁, II₂, and III.

The rock samples in the chromatographic experiment were firstly extracted with trichloromethane by a conventional Soxhlet extractor for seventy-two hours, and the asphaltenes were precipitated by petroleum ether. The

TABLE 1: Characteristics of organic geochemistry and biomarker of the source rocks in well J31, Sichuan Basin.

Member	Depth (m)	TOC	S ₁ +S ₂	Ro	Pr/Ph
Mb. 5	2821.1	1.17	1.06	1.28	1.01
Mb. 5	2833.21	1.31	1.83	1.28	0.97
Mb. 5	2866.12	0.97	0.78	1.30	1.11
Mb. 5	2901.12	0.92	0.15	1.32	0.98
Mb. 5	2923.53	1.42	2.87	1.33	1.07
Mb. 5	2935.91	1.12	0.43	1.33	1.07
Mb. 5	3001.72	1.61	7.40	1.36	0.65
Mb. 5	3003.11	1.73	6.11	1.36	0.65
Mb. 5	3005.51	1.82	5.17	1.36	0.67
Mb. 5	3007.92	1.67	3.32	1.36	0.65
Mb. 5	3010.31	2.08	6.51	1.36	0.71
Mb. 5	3015.72	1.63	6.23	1.36	0.72
Mb. 5	3025.11	1.66	6.06	1.36	0.72
Mb. 5	3031.12	1.62	4.62	1.37	0.75
Mb. 5	3035.14	1.47	4.57	1.37	0.76
Mb. 5	3037.32	1.97	8.31	1.40	0.78
Mb. 5	3039.45	1.77	9.78	1.40	0.71
Mb. 4	3042.14	0.59	0.27	1.40	1.35
Mb. 4	3087.32	0.61	0.32	1.38	1.35
Mb. 3	3182.12	1.71	6.09	1.42	0.77
Mb. 3	3194.11	1.63	7.73	1.42	0.76
Mb. 3	3216.52	1.91	5.47	1.44	0.73
Mb. 3	3247	2.06	8.26	1.44	0.65
Mb. 3	3263	1.67	7.33	1.51	0.66
Mb. 3	3291	1.71	6.39	1.78	0.67
Mb. 1	3373	0.98	1.12	1.81	0.92
Mb. 1	3386	0.93	1.83	1.86	0.97
Mb. 1	3393	0.88	1.39	1.87	1.03

extracted liquid was then placed in the chromatographic column in which silica gel and aluminum oxide were mixed in a 3:2 ratio. The liquid in the column was rinsed with n-hexane to obtain the saturated hydrocarbons, aromatic hydrocarbons, and nonhydrocarbons. The chromatographic and chromatographic values of saturated hydrocarbons were determined by separating the saturated hydrocarbons. The chromatographic column was the SE-54 quartz elastic capillary column with a length of 30 m and a shunt ratio of 20:1. The heating process of saturated hydrocarbon was as follows: the temperature was kept constant for 2 min with the initial temperature (10°C), and the final temperature was kept constant for 30 min with the heating rate (4°C/min from 10°C to 220°C; 2°C/min from 220°C to 300°C). The conditions of mass spectrometry were as follows: ion source display temperature 180°C, ionization energy 70 eV, interfacial furnace temperature 275°C, and mass scanning range 50-550 m/z.

3.3. Major and Trace Elements. Major elements were tested at the Australian Mineral Laboratory in Australia. The ele-

ments were determined using the ME-XRF26 X-ray fluorescence (XRF) spectrometer. First, two samples were weighed. A sample was fully mixed with a nitrate lithium borate-lithium nitrate melt flux containing lithium nitrate and then melted at high temperature. The melt was poured into a platinum mould to form a flat glass sheet and analyzed using an XRF spectrometer. Simultaneously, the other sample was placed in a muffle furnace and burned at 1000°C. Subsequently, it was cooled and weighed. The weight difference was due to the burning loss before and after heating. The total content was obtained by adding the loss of combustion results to the element oxide results measured by XRF.

Trace elements were also tested at the Australian Mineral Laboratory. Ultratrace elements and rare earth elements were determined by Inductively Coupled Plasma-Atomic Emission Spectroscopy (ICP-AES) and mass spectrometry (MS) using ME-MS61R digestion. The samples were first digested with perchloric acid, nitric acid, hydrofluoric acid, and hydrochloric acid, then diluted with dilute hydrochloric acid, and analyzed by ICP-AES. If the Bi/Hg/Mo/Ag/W ratio was high, the sample was diluted accordingly and then analyzed by ICP-MS. The final analysis result was obtained by correcting the spectral interference between the elements.

4. Results

4.1. Geochemical Characteristics of Source Rocks. There are differences between TOC and S₁+S₂ in the 1st, 3rd, and 5th Mbs. source rocks (Table 1). The TOC and S₁+S₂ of the source rocks in Mb. 1 are 0.88%-2.08% and 0.15 mg/g-9.78 mg/g, respectively (Table 1). The source rocks in Mb. 3 have the highest TOC and S₁+S₂ content with an average of 1.78% and 6.88 mg/g, respectively. The TOC and S₁+S₂ of the 3rd Mb. source rocks are relatively low with an average of 1.53% and 4.42 mg/g. The TOC and S₁+S₂ of the 3rd Mb. source rocks are the lowest with an average of 0.93% and 1.45 mg/g. The organic matter types are featured with type II₂ and type III in the Xujiahe source rocks (Table 2; Figure 2). The organic matter types are type II₂ in the source rocks from Mb. 1 and Mb. 3, and the organic matter is typed II₂ and III in the 5th Mb. source rocks. The Ro values of the Xujiahe source rocks range from 1.28% to 1.87% (Table 1). The average Ro values are 1.85%, 1.50%, and 1.35%, respectively, in the 1st, 3rd, and 5th Mbs. source rocks.

4.2. Biomarker Characteristics of Source Rocks. The source rocks were characterized by low Pr/Ph ratios and abundant dinosteranes in the study area. A Pr/Ph ratio was commonly used to reflect the sedimentary environment of source rocks [42]. The Pr/Ph ratio was less than 1 in the marine or lacustrine source rocks [43]. In contrast, the Pr/Ph ratio was greater than 2 in the coal-bearing source rocks of the swamp environment [44]. The Pr/Ph values are mainly less than 1 in the Xujiahe source rocks (Table 1), ranging from 0.65 to 1.11 (average = 0.81), and the Pr/Ph values of 65.38% of source rocks are distributed in 0.6-0.8. The Pr/Ph values of few samples are greater than 1 (Table 1). N-alkanes have a bimodal distribution and abundant n-alkanes with low

TABLE 2: Kerogen macerals of the Xujiahe coal-bearing source rocks in well J31, Sichuan Basin.

Depth (m)	Member	Kerogen maceral content (%)				TI value	Type
		Liptinite	Exinite	Vitrinite	Inertinite		
2833.21	Mb. 5	28	/	22	50	-38.50	III
2901.12	Mb. 5	23	/	29	48	-46.75	III
3031.12	Mb. 5	58	/	13	29	19.25	II ₂
3039.45	Mb. 5	47	/	29	24	1.25	II ₂
3182.12	Mb. 3	60	/	17	23	24.25	II ₂
3247.19	Mb. 3	62	/	12	26	27	II ₂
3263.27	Mb. 3	48	/	22	30	1.5	II ₂
3386.83	Mb. 1	55	/	16	29	14	II ₂

TABLE 3: Major element values (%) of the Xujiahe coal-bearing source rocks in well J31, Sichuan Basin.

Member	Depth (m)	SiO ₂	TiO ₂	Al ₂ O ₃	Fe ₂ O ₃	MnO	MgO	CaO	Na ₂ O	K ₂ O	P ₂ O ₅	Ca	Na	Mg	Al	P	Ti	K
Mb. 5	2821.1	57.36	0.61	17.25	5.75	0.10	2.57	2.82	0.26	2.85	0.10	2.01	0.19	1.54	9.13	0.05	0.36	2.36
Mb. 5	2833.21	51.62	0.65	17.31	7.00	0.16	2.62	4.65	0.26	3.17	0.12	3.32	0.19	1.57	9.16	0.05	0.39	2.63
Mb. 5	2866.12	51.11	0.52	17.75	5.82	0.08	2.69	9.72	0.27	2.99	0.05	6.94	0.20	1.61	9.40	0.02	0.31	2.48
Mb. 5	2901.12	54.23	0.69	12.03	4.36	0.06	5.80	9.82	0.22	1.62	0.07	7.01	0.16	3.48	6.37	0.03	0.42	1.34
Mb. 5	2933.53	56.18	0.60	20.87	5.40	0.02	2.13	0.27	0.34	3.99	0.07	0.19	0.25	1.28	11.05	0.03	0.36	3.31
Mb. 5	2965.91	52.44	0.67	18.90	4.70	0.02	1.76	10.29	0.25	2.42	0.10	7.35	0.18	1.05	10.00	0.04	0.40	2.00
Mb. 5	3001.72	34.46	0.55	10.99	4.75	0.13	4.11	18.83	0.19	2.18	0.13	13.45	0.14	2.46	5.82	0.06	0.33	1.81
Mb. 5	3003.11	36.96	0.63	11.49	4.85	0.11	5.00	15.90	0.19	2.26	0.11	11.36	0.14	3.00	6.08	0.05	0.38	1.87
Mb. 5	3005.51	33.44	0.57	10.70	4.83	0.13	4.37	18.73	0.18	2.12	0.12	13.38	0.13	2.62	5.67	0.05	0.34	1.76
Mb. 5	3007.92	56.96	0.70	19.76	6.63	0.07	2.14	0.56	0.33	3.81	0.09	0.40	0.25	1.28	10.46	0.04	0.42	3.17
Mb. 5	3010.31	82.78	0.17	7.81	2.06	0.01	0.51	0.29	1.03	1.94	0.04	0.21	0.76	0.31	4.14	0.02	0.10	1.61
Mb. 5	3015.72	47.68	0.69	15.16	4.84	0.08	3.61	6.20	0.25	3.04	0.12	4.43	0.18	2.17	8.03	0.05	0.41	2.52
Mb. 5	3025.11	36.37	0.59	12.18	23.92	1.23	1.26	1.94	0.25	2.40	0.11	1.38	0.18	0.76	6.45	0.05	0.36	1.99
Mb. 5	3031.12	57.86	0.61	19.83	6.36	0.08	1.92	0.28	0.33	3.72	0.07	0.20	0.25	1.15	10.50	0.03	0.37	3.08
Mb. 5	3035.14	56.85	0.78	14.06	4.61	0.05	3.21	5.07	0.24	1.81	0.11	3.62	0.18	1.93	7.44	0.05	0.47	1.50
Mb. 5	3037.32	62.79	0.91	18.20	5.43	0.06	1.84	0.37	0.29	3.59	0.06	0.26	0.21	1.10	9.64	0.03	0.55	2.98
Mb. 5	3039.45	56.46	0.72	13.81	6.05	0.11	3.16	4.47	0.58	2.74	0.13	3.20	0.43	1.90	7.31	0.05	0.43	2.27
Mb. 4	3042.14	72.14	0.40	11.12	3.26	0.06	1.33	1.36	1.11	2.60	0.07	0.97	0.82	0.80	5.88	0.03	0.24	2.16
Mb. 4	3087.32	57.68	0.77	15.23	6.07	0.07	3.29	2.32	0.49	7.06	0.13	1.66	0.36	1.97	8.06	0.05	0.46	5.86
Mb. 3	3182.12	25.35	0.36	12.06	4.86	0.13	4.44	16.82	0.16	2.52	0.07	12.01	0.12	2.66	6.39	0.03	0.22	2.09
Mb. 3	3194.11	25.84	0.33	7.95	3.59	0.19	4.86	25.71	0.12	1.70	0.07	18.37	0.09	2.92	4.21	0.03	0.20	1.41
Mb. 3	3216.52	28.11	0.39	6.87	3.06	0.19	5.36	25.61	0.11	2.62	0.09	18.29	0.08	3.22	3.64	0.04	0.24	2.17
Mb. 3	3247.19	38.36	0.41	8.32	3.93	0.16	4.82	26.78	0.09	3.12	0.12	19.13	0.07	2.89	4.40	0.05	0.25	2.59
Mb. 3	3263.27	27.53	0.36	9.37	3.67	0.16	4.75	24.77	0.11	2.53	0.08	17.69	0.08	2.85	4.96	0.03	0.22	2.10
Mb. 3	3291.26	28.12	0.32	11.23	3.55	0.19	4.81	18.92	0.11	3.02	0.07	13.51	0.08	2.89	5.95	0.03	0.19	2.51
Mb. 1	3373.47	53.67	0.98	16.38	6.89	0.13	3.13	5.92	0.67	2.84	0.23	4.23	0.50	1.88	8.67	0.10	0.59	2.35
Mb. 1	3386.83	52.23	1.00	17.21	6.32	0.09	3.24	6.13	0.59	3.03	0.20	4.38	0.44	1.94	9.11	0.09	0.60	2.51
Mb. 1	3393.81	51.70	0.89	17.14	5.89	0.11	3.07	6.40	0.55	2.32	0.19	4.57	0.41	1.84	9.07	0.08	0.53	1.93

carbon numbers (Figure 3). The dinosterane is also known as 4,23,24-trimethyl cholestane. The peak sequence of the dinosterane with strong M/Z 213 fragments is located after C₂₉ sterane with 8 isomers [45]. Figure 4 shows that the source rocks contain the high dinosteranes in the Mb. 1, Mb. 3, and Mb. 5.

4.3. Major Element Geochemistry. The main average enriched oxides are SiO₂ (46.79%), Al₂O₃ (14.02%), CaO (10.30%), Fe₂O₃ (5.74%), K₂O (3.06%), and MgO (3.35%) in the Xujiahe Formation. The contents of MnO, P₂O₅, Na₂O, and TiO₂ are less than 1.5% (Table 3). Compared with high-quality oil-bearing source rocks, the Xujiahe

TABLE 4: Trace elements (ppm) of the Xujiahe coal-bearing source rocks in well J31, Sichuan Basin.

Member	Depth (m)	Ba/Al	P/Ti	Sr/Cu	C	U/Th	V/(V+Ni)	Sr/Ba	Rb/K	CIA	(La/Yb) _N	Zr/Rb	Zr/Al	Ba _(bio)
Mb. 5	2821.1	58.19	0.12	4.16	1.60	0.23	0.70	0.25	70.34	72.91	16.57	1.49	27.11	531.21
Mb. 5	2833.21	62.14	0.13	4.97	2.43	0.21	0.71	0.29	70.27	66.73	15.88	1.25	25.20	569.13
Mb. 5	2866.12	55.60	0.07	3.62	1.19	0.22	0.72	0.23	67.44	56.83	16.12	1.52	27.09	522.57
Mb. 5	2901.12	52.92	0.08	4.98	1.41	0.27	0.71	0.24	66.02	48.71	15.41	1.82	25.36	337.05
Mb. 5	2933.53	59.10	0.09	3.37	0.64	0.28	0.74	0.21	72.10	79.79	20.57	0.98	21.19	652.97
Mb. 5	2965.91	52.70	0.11	3.51	0.81	0.25	0.68	0.23	67.04	57.68	16.68	1.84	24.72	526.93
Mb. 5	3001.72	73.77	0.17	11.16	1.76	0.25	0.62	0.53	62.59	33.75	15.26	1.57	30.58	429.30
Mb. 5	3003.11	75.15	0.12	7.22	1.55	0.26	0.63	0.41	61.11	38.03	15.97	1.63	30.70	456.87
Mb. 5	3005.51	73.42	0.15	7.27	1.89	0.26	0.66	0.53	64.96	33.36	15.68	1.63	32.78	416.25
Mb. 5	3007.92	53.79	0.10	3.22	1.29	0.22	0.74	0.20	65.71	78.67	17.94	1.21	24.06	562.56
Mb. 5	3010.31	97.61	0.18	17.62	0.36	0.22	0.61	0.17	38.05	68.54	29.88	2.37	35.15	404.07
Mb. 5	3015.72	65.94	0.13	5.20	1.30	0.22	0.68	0.34	65.53	60.27	19.95	1.26	25.91	529.44
Mb. 5	3025.11	77.77	0.14	3.25	17.13	0.30	0.67	0.27	84.67	70.97	11.49	1.14	29.75	501.57
Mb. 5	3031.12	62.10	0.08	5.26	1.23	0.30	0.71	0.20	73.52	80.02	17.91	1.12	24.19	651.97
Mb. 5	3035.14	59.47	0.11	3.42	1.22	0.26	0.63	0.28	75.57	63.27	15.78	1.86	28.34	442.40
Mb. 5	3037.32	64.93	0.05	5.19	0.96	0.32	0.70	0.18	69.06	80.05	16.66	1.25	26.71	625.85
Mb. 5	3039.45	71.73	0.13	1.23	1.72	0.21	0.55	0.21	53.99	62.60	14.51	2.18	36.56	524.29
Mb. 4	3042.14	44.67	0.13	12.44	1.24	0.22	0.50	0.19	42.42	69.22	22.54	2.49	38.75	262.62
Mb. 4	3087.32	39.05	0.12	4.58	2.48	0.24	0.48	0.23	31.97	69.52	15.73	1.62	37.63	314.68
Mb. 3	3182.12	81.22	0.14	10.94	1.67	0.28	0.55	0.41	64.61	37.72	16.86	1.27	26.82	518.96
Mb. 3	3194.11	112.98	0.15	12.83	2.67	0.25	0.50	0.73	57.12	22.23	14.61	1.67	31.98	475.62
Mb. 3	3216.52	132.16	0.18	18.02	3.14	0.24	0.62	0.86	60.49	20.08	14.08	1.16	41.83	481.05
Mb. 3	3247.19	133.99	0.21	15.33	3.04	0.28	0.63	0.79	56.37	22.31	15.34	1.32	43.82	589.52
Mb. 3	3263.27	111.59	0.16	16.57	2.89	0.27	0.62	0.83	58.31	25.94	14.83	1.43	35.33	553.43
Mb. 3	3291.26	84.40	0.17	15.32	2.73	0.28	0.58	0.76	57.62	34.89	14.32	1.31	31.80	502.16
Mb. 1	3373.47	57.83	0.17	5.86	1.37	0.24	0.46	0.36	54.85	61.49	18.31	1.86	27.69	501.32
Mb. 1	3386.83	56.33	0.15	6.07	1.43	0.25	0.47	0.37	55.23	62.54	17.68	1.73	26.37	513.10
Mb. 1	3393.81	54.99	0.15	6.18	1.52	0.25	0.46	0.39	56.85	62.03	17.97	1.92	23.21	498.69

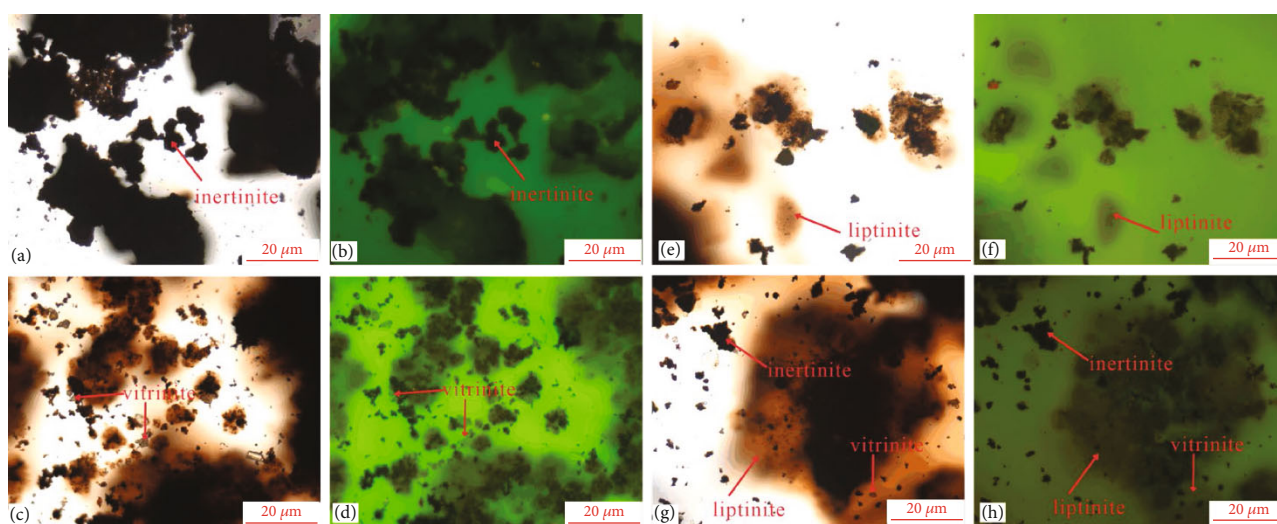


FIGURE 2: Fluorescence images of the kerogens in the Xujiahe coal-bearing source rocks of well J31, Sichuan Basin. (a) Transmitted light, 2833.21 m, 1×500 , SSCS; (b) fluorescence, 2833.21 m, 1×500 , SSCS; (c) transmitted light, 3031.12 m, 1×500 , FSCS; (d) fluorescence, 3031.12 m, 1×500 , FSCS; (e) transmitted light, 3182.12 m, 1×500 , SSTS; (f) fluorescence, 3182.12 m, 1×500 , SSTS; (g) transmitted light, 3386.83 m, 1×500 , FSTS; (h) fluorescence, 3396.83 m, 1×500 , FSTS.

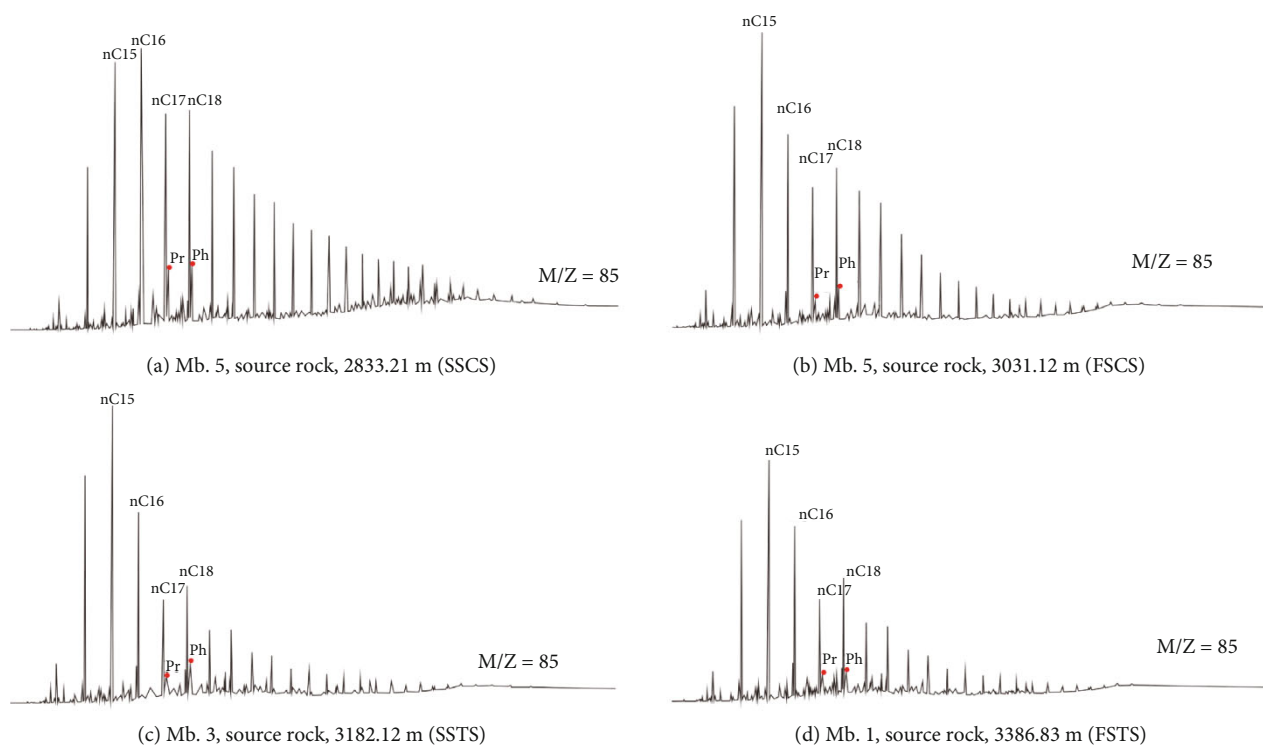


FIGURE 3: Chromatograms of source rocks in well J31, Sichuan Basin.

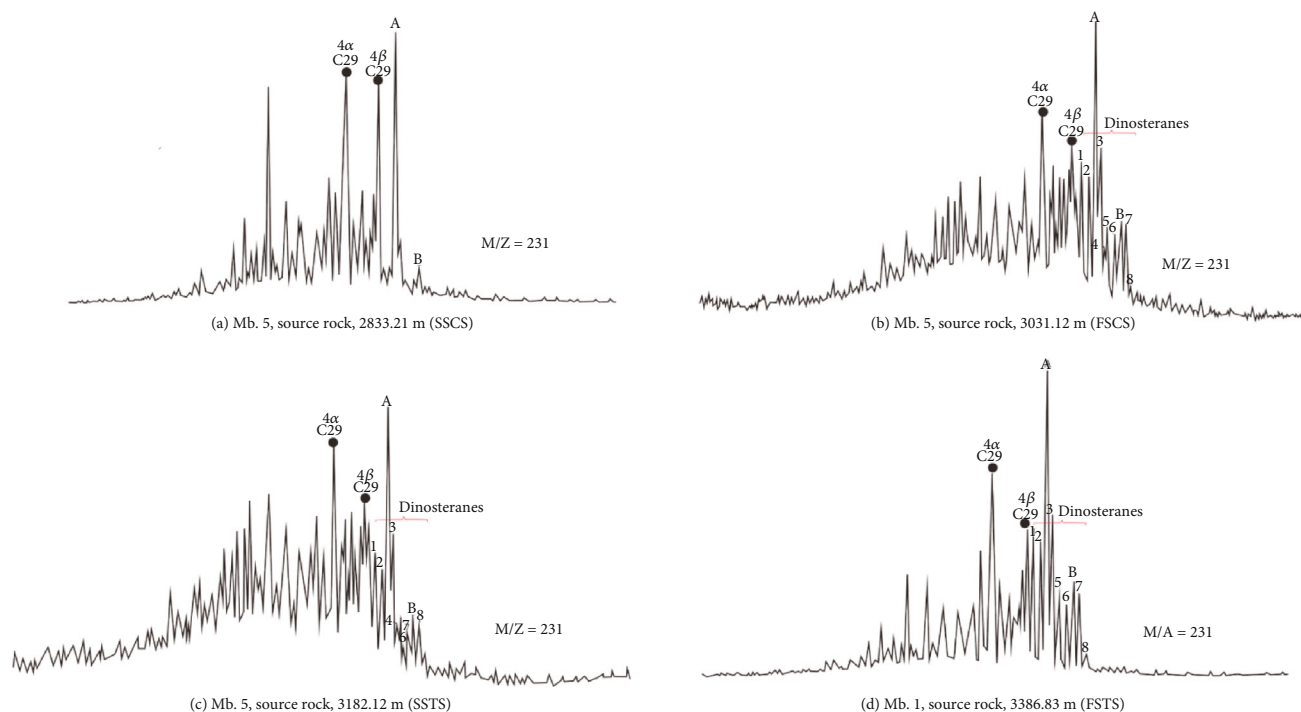


FIGURE 4: Mass spectrograms of dinosteranes in the source rocks of well J31, Sichuan Basin. A: 4α -Methyl, 24-ethyleholestane; B: 4β -methyl, 24-ethyleholestane; 1: $4\alpha,23S,2S$ -trimethyleholestane; 2: $4\alpha,23S,24R$ -trimethyleholestane; 3: $4\alpha,23R,24R$ -trimethyleholestane; 4: $4\alpha,23R,24S$ -trimethyleholestane; 5: $4\beta,23S,24S$ -trimethyleholestane; 6: $4\beta,23S,24R$ -trimethyleholestane; 7: $4\beta,23R,24R$ -trimethyleholestane; 8: $4\beta,23R,24S$ -trimethyleholestane.

coal-bearing source rocks have higher CaO, Fe_2O_3 , and MgO contents and lower contents of other oxides (Figure 5).

In contrast, the Mb. 3 has a high average content of CaO (23.10%) and a relatively low content of terrestrial minerals (Al_2O_3 , Fe_2O_3 , MgO, K_2O , and SiO_2). The Mb.

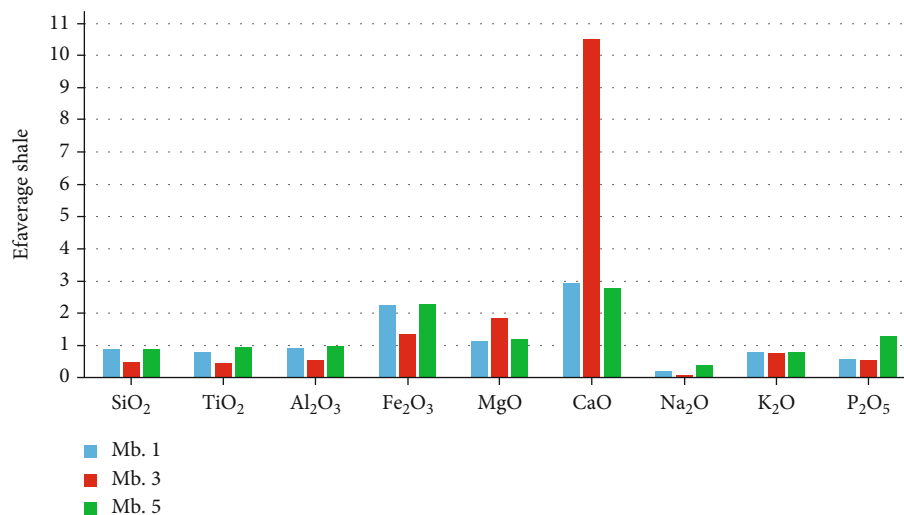


FIGURE 5: Distribution of major elements in different coal-bearing source rocks, Sichuan Basin. Note: distribution of major elements: the ratio of major elements of Xujiahe coal-bearing source rocks to high-quality oil-bearing source rocks. Average shale composition from Wedepohl [88, 89].

1 and Mb. 3 have a low content of CaO (6.15% and 6.48%) and high terrestrial minerals. The inverse ratio between CaO and terrestrial minerals indicates that the CaO is not exotic but an authigenic mineral in the basin.

4.4. Trace Element Geochemistry. The average trace elements are Mn (1205 ppm), Ba (496 ppm), Zr (213 ppm), Sr (191 ppm), Rb (143 ppm), V (102 ppm), Cr (105 ppm), Ce (75 ppm), Zn (64.4 ppm), and Ni (63.5 ppm) in the Xujiahe Formation. The trace element content of other elements is less than 50%. Compared with high-quality oil-bearing source rocks, the Xujiahe source rocks are more enriched in Cr, Mn, Cs, and Zr (Figure 6). The contents of other trace elements are lower than those of oil-bearing source rocks.

In contrast, the 1st and 5th Mbs. source rocks are more enriched in Be, V, Cu, Zn, Ga, Rb, Y, Nb, Zr, Cs, La, Ce, and Cd. Additionally, the 3rd Mb. source rocks have higher Co, Sr, and Mo contents. The enrichment degrees of Cr, Mn, and Ba are similar in three Xujiahe source rocks.

5. Discussion

5.1. Palaeoproductivity. Biological productivity referred to as the rate of carbon sequestration by photosynthesis plays an essential role in the organic matter enrichment [46]. Elements sensitive to productivity include Ba, Cu, Ni, Cd, and Zn. Moreover, palaeoproductivity is positively correlated with organic matter enrichment [46–48]. $Ba_{(bio)}$ can be regarded as an indicator of productivity [49, 50]. $Ba_{(bio)} = B a_{(total)} - (Al \times Ba/Al_{al\text{silicate}})$; $Ba/Al_{al\text{silicate}} = 0.0075$ [21, 51, 52]. Thus, $Ba_{(bio)}$ can exclude the impact of abiotic Ba on the index. As Ba is usually precipitated as biological barite, barite is relatively stable under oxidation conditions and readily soluble under reduction conditions. Attention should be paid to the impact of the sedimentary environment on the Ba accuracy in representing productivity. Moreover, the

enrichment of Ba, Cu, and other vital elements is controlled by lithology. Therefore, these elements need to be corrected in the productivity evaluation. As an important component of organisms, P is enriched in sediments in the form of organic complexation to represent productivity [53]. In short, the enrichment coefficients of P/Al or P/Ti, rather than the content of these elements, are often used to describe the palaeoproductivity to eliminate the influence of changes in lithology and clastic composition.

Ba/Al, $Ba_{(bio)}$, and P/Ti are used to describe the palaeoproductivity in the work. As presented in Table 4, the average $Ba_{(bio)}$ value of the Xujiahe source rocks is 512.24 ppm (~337.05–652.97 ppm), and the average Ba/Al content is 74.69 (~52.70–133.99). The $Ba_{(bio)}$ content ranges from 1000 ppm to 5000 ppm in the high-productivity areas of the modern equatorial Pacific [54]. The biological productivity of the Xujiahe source rocks is at a medium palaeoproductivity level (200–1000 ppm). The average P/Ti value is 0.13 (~0.05–0.21) in the Xujiahe source rocks. However, the ratio of P/Ti is much lower than that of highly productive regions of the modern equatorial Pacific (~2–8) [54]. Furthermore, the P element may be influenced by the redox degree of pore water (oxidation to secondary oxidation conditions promote its retention) and the availability of adsorbed iron when representing palaeoproductivity. In contrast, biological productivity is the highest in the 3rd Mb. source rocks, with the average of $Ba_{(bio)}$ and Ba/Al values reaching 520.13 ppm and 109.39, respectively, followed by those of the 5th Mb. source rocks (average $Ba_{(bio)}=510.85$ ppm; Ba/Al = 65.67). The 1st Mb. source rocks have the lowest biological productivity (average $Ba_{(bio)}=504.37$ ppm; Ba/Al = 56.38).

A positive correlation was found between TOC and palaeoproductivity from the Xujiahe source rocks (Figure 7). Therefore, palaeoproductivity is the main controlling factor affecting organic matter enrichment in the Xujiahe coal-bearing source rocks.

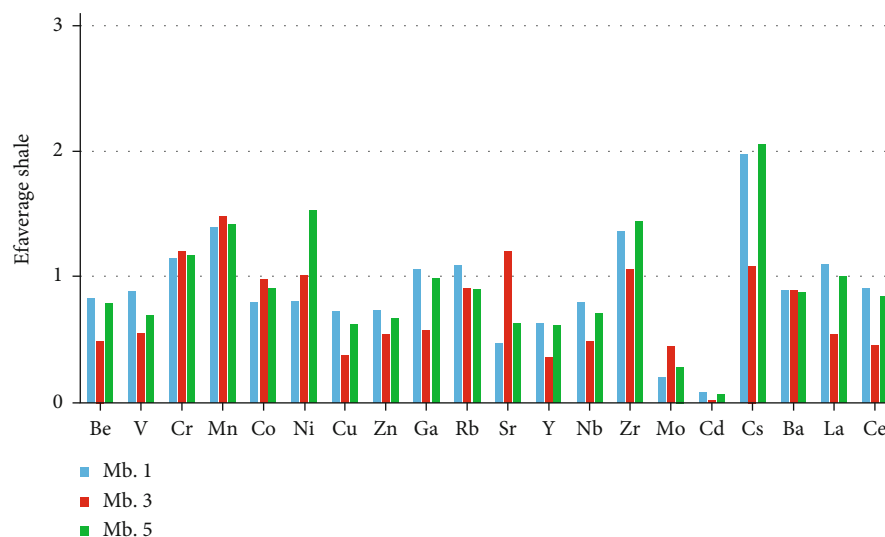


FIGURE 6: Distribution of trace elements in different coal-bearing source rocks, Sichuan Basin. Note: distribution of trace elements: the ratio of trace elements of Xujiahe coal-bearing source rocks to high-quality oil-bearing source rocks. Average shale composition from Wedepohl [88, 89].

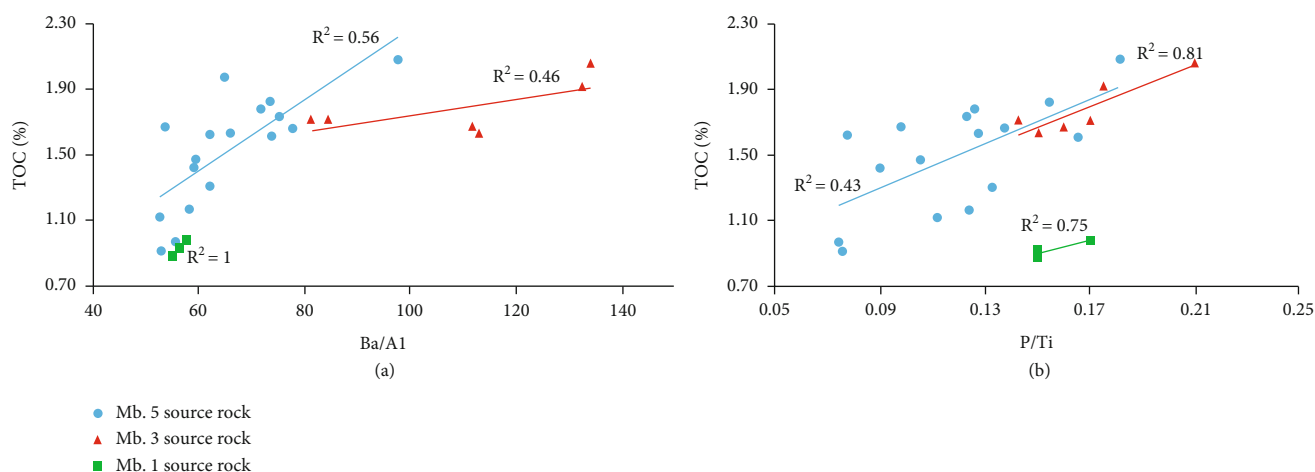


FIGURE 7: Cross plot of biological productivity parameters (Ba/Al and P/Ti) and TOC. TOC is positively correlated with Ba/Al and P/Ti.

5.2. Palaeoenvironment

5.2.1. Palaeoclimate Conditions. Changes in the composition and relative content of sediments can reflect climatic characteristics [55]. Fe, Mn, Cr, Ni, V, and Co are enriched in wet conditions, while Ca, Mg, Sr, Ba, K, and Na are more enriched in dry conditions. Zhao et al. [56] established a palaeoclimate index ($C = \frac{\sum(\text{Fe} + \text{Mn} + \text{Cr} + \text{Ni} + \text{V} + \text{Co})}{\sum(\text{Ca} + \text{Mg} + \text{Sr} + \text{Ba} + \text{K} + \text{Na})}$). However, it is still debatable whether the threshold established in the Junggar Basin can be applied to the Sichuan Basin. The climate is correspondingly divided into arid ($C < 0.2$), semiarid ($0.2 \leq C < 0.4$), subhumid ($0.4 \leq C < 0.6$), subhumid ($0.6 \leq C < 0.8$), and humid ($C \geq 0.8$), according to the C values [21, 35]. Additionally, the Sr/Cu ratio is used to evaluate the palaeoclimate. A Sr/Cu ratio between 1 and 10 indicates a warm

and wet climate, and that greater than 10 indicates an arid climate [57].

The ratio of Sr/Cu is between 1.23 and 18.02, and the C value is between 0.36 and 17.13 in the Xujiahe Formation (Table 4). This indicates that the climate change of the Xujiahe Formation is relatively frequent, and both arid and humid climates exist. The average Sr/Cu and C values of the Mb. 5 are 5.57 and 2.26, respectively, indicating a humid climate. The average Sr/Cu value is 14.83 in the Mb. 3, indicating an arid climate, whereas the C value is 2.69, indicating a humid climate. The increase in the C value may be caused by the enrichment degree of various elements in the oxygen-rich sedimentary environment. The high salinity of the Mb. 3 is also caused by climate drought, which would be discussed in Section 5.2.3 (Table 4). The average Sr/Cu and C values are 6.04 and 1.44 in the Mb. 1, indicating a humid climate (Table 4).

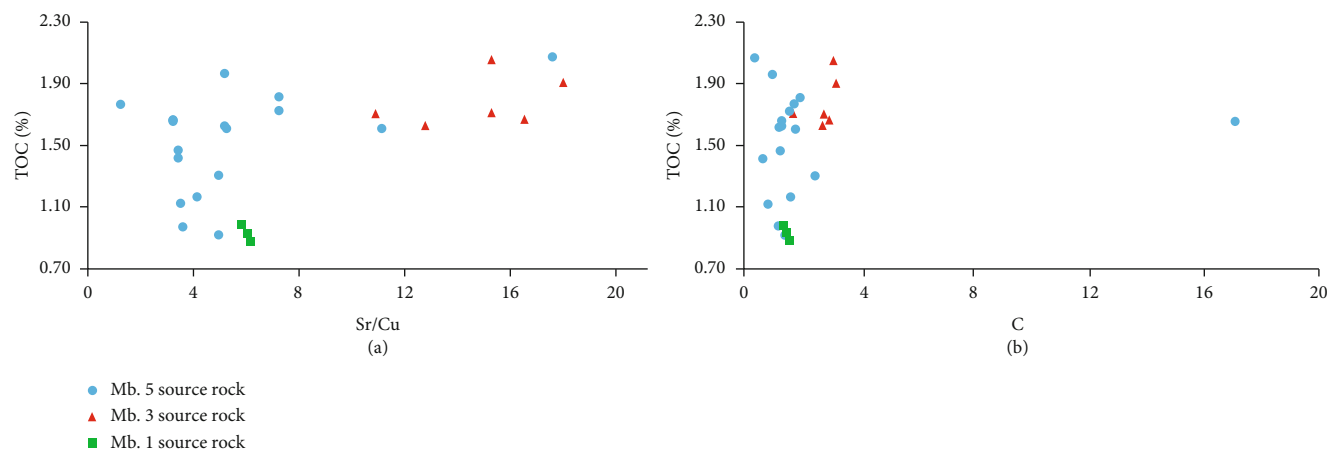


FIGURE 8: Cross plot of paleoclimate parameters (Sr/Cu and C) and TOC. TOC does not correlate with Sr/Cu and C.

Additionally, we did not find a correlation between palaeoclimate indicators and TOC in the cross plot (Figure 8). Therefore, the palaeoclimate is not the main controlling factor affecting organic matter enrichment in the Xujiahe coal-bearing source rocks.

5.2.2. Redox Conditions and Palaeowater Depth. The Th content is barely affected by redox conditions in the water. The U/Th ratio is used to reflect the redox conditions of the water. A U/Th ratio lesser than 0.75 indicates water oxidation, a U/Th ratio (0.75-1.25) suggests a transitional environment, and a U/Th ratio greater than 1.25 suggests an oxygen-deficient environment [58]. Additionally, V and Ni are preferentially enriched in anoxic water, and $V/(V + Ni)$ can be used to evaluate the palaeoenvironment [59]. A $V/(V + Ni)$ ratio greater than 0.77 indicates stratification and reducibility, while a $V/(V + Ni)$ ratio below 0.6 indicates weak stratification and an oxygen-rich environment [60]. Moreover, Rb can easily be deposited in a low-energy environment. Rb/K reflects the water depth. The higher the Rb/K value, the deeper the water is [21].

The average values of U/Th and $V/(V + Ni)$ are 0.25 (~0.21-0.32) and 0.63 (~0.46-0.74), respectively, in the Xujiahe Formation. This shows that the water was oxidized to a high degree in the Xujiahe period, belonging to a semi-oxidized and oxidized sedimentary environment. The average values of U/Th and $V/(V + Ni)$ values are 0.25/0.46, 0.27/0.58, and 0.25/0.67, respectively, in the 1st, 3rd, and 5th Mbs. (Table 4). The average Rb/K values are 55.64, 59.09, and 66.35, respectively, in the 1st, 3rd, and 5th Mbs. (Table 4). Therefore, the Xujiahe Formation is an evolutionary process wherein the reducibility of water became stronger and the water gradually deepens from Mb. 1 to Mb. 5.

The U/Th, $V/(V + Ni)$, and Rb/K did not correlate with TOC in the cross plot (Figures 9(a)–9(c)). This shows that redox conditions and water depth are not the main controlling factors affecting organic matter enrichment in the Xujiahe coal-bearing source rocks.

5.2.3. Salinity Conditions. Strontium (Sr) and barium (Ba) are widely distributed in the crust and exist in the water in

the form of bisulfates. When the salinity of water gradually increases, Ba first precipitates in the form of barium sulfate, followed by Sr in the form of strontium sulfate [61]. The Sr/Ba ratio reflects the salinity of the water. The higher the Sr/Ba ratio, the higher the salinity of the water is. A Sr/Ba ratio lesser than 1 represents a freshwater environment and vice versa [62, 63]. The average value of Sr/Ba is 0.40 (~0.17-0.86) in the Xujiahe Formation, indicating that the water comprised freshwater to brackish water environments in the Xujiahe Formation. The average Sr/Ba values were 0.37, 0.73, and 0.28, respectively, in the 1st, 3rd, and 5th Mbs. (Table 4). The water salinity was variable in the Xujiahe Formation. The water became saltier during the 1st and 3rd Mbs. sedimentary periods under the background of a freshwater sedimentary environment.

Additionally, there was no significant correlation between palaeosalinity index and TOC (Figure 9(d)). Therefore, the palaeosalinity of water is not the main controlling factor affecting organic matter enrichment in the Xujiahe coal-bearing source rocks.

5.2.4. Weathering Conditions. The chemical index of alteration (CIA) reflects the weathering degree and palaeoclimate of the source area. CIA is defined as $[(Al_2O_3)/(Al_2O_3 + Na_2O + CaO + K_2O)] \times 100$. Furthermore, Deng et al. [35] reviewed the most detailed and widely accepted chemical weathering indices and suggested that the classical CIA values were affected by nonweathering factors such as the sedimentary cycle, hydrodynamic sorting, diagenetic alteration (especially illite), and little provenance lithologic transformation by applying the CIA index to the study of the Xujiahe black shale. Therefore, conventional default CIA values are not recommended to evaluate the degree of weathering and palaeoclimate without identification and correction. Yang et al. [64] directly used CIA values and proposed that the climate is hot and humid (high CIA) in the 1st, 3rd, and 5th Mbs. deposition periods, while that is cold and dry (low CIA) in the 2nd, 4th, and 6th Mbs. deposition periods. This perspective should not be accepted because the CIA index might be more obviously controlled by the grain size rather than climate. Moreover, Xu et al. [65] also

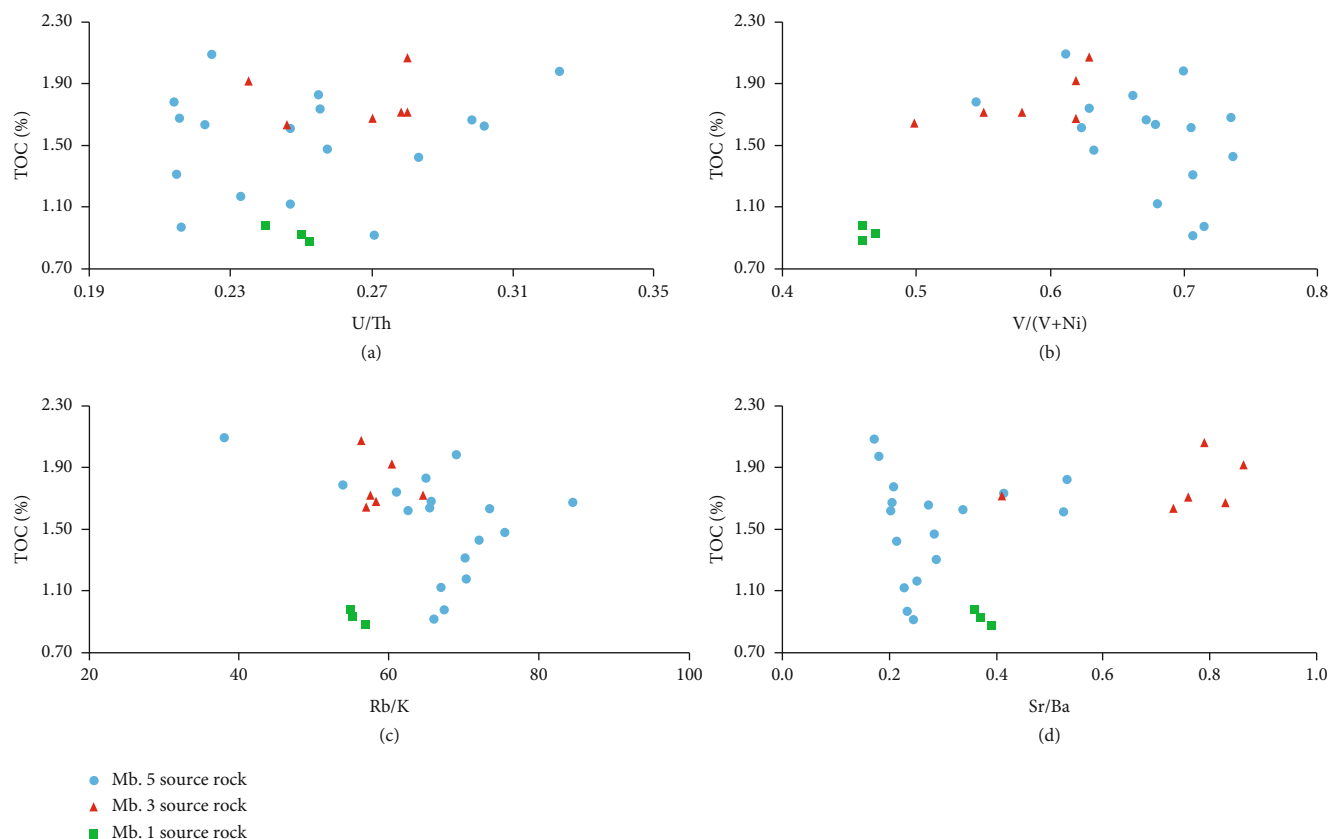


FIGURE 9: Cross plot of TOC with (a, b) redox, (c) water depth, and (d) salinity. TOC does not correlate with redox, water depth, and salinity.

found that the Xujiache sedimentary period is characterized by a humid and hot tropical-subtropical climate based on pollen and clay mineral analysis. The average CIA of the Mb. 3 (27.20) is lower than those of the Mb. 1 and Mb. 5, which may be influenced by the grain size, hydrodynamic conditions, and lithology in the sedimentary period (Table 4). The CIA cannot be applied to evaluate the weathering of the source area in the study area. Moreover, the ratio of rare earth elements can also determine the degree of weathering. $(La/Yb)_N$ was positively correlated with the degree of weathering [21]. This parameter provides reliable evaluation to evaluate the degree of weathering.

The average value of $(La/Yb)_N$ is 16.78 (~11.49-29.88) in the Xujiache sediments (Table 4). This shows that the Xujiache sediments experienced moderate to high weathering. The average values of $(La/Yb)_N$ are 17.99, 15.01, and 17.19 in the 1st, 3rd, and 5th Mbs. sediments. These results show that the weathering intensity decreases initially and then increases from Mb. 1 to Mb. 5, and the weathering is the weakest in the Mb. 1.

There was no significant correlation between weathering index and TOC (Figure 10(a)). Weathering conditions are not the main controlling factors affecting organic matter enrichment in the Xujiache coal-bearing source rocks.

5.2.5. Terrestrial Inputs and Hydrodynamic Conditions. Stable terrestrial elements (TiO_2 and Al_2O_3) have indicated ter-

restrial inputs [66]. Moreover, other terrestrial elements (K_2O , Na_2O , and SiO_2) were positively correlated with TiO_2 and Al_2O_3 [67]. The Zr element with stable chemical properties reacts well with hydrodynamic conditions [68]. High Zr content is mainly formed in the strong hydrodynamic sedimentary environment [68]. However, Rb is characterized by low-energy sedimentary environments because it is deposited mainly in silicates at low energies. A higher Zr/Rb ratio implies strong hydrodynamic conditions [69, 70].

In contrast, the content of terrestrial inputs is the highest in the Mb. 1 with SiO_2 and TiO_2 accounting for 52.53% and 0.75%, respectively, followed by the Mb. 5 ($SiO_2 = 52.09%$ and $TiO_2 = 0.63%$). The content of terrestrial inputs is the lowest in the Mb. 3 with SiO_2 and TiO_2 accounting for 28.89% and 0.36%, respectively, (Table 3). The average Zr/Rb values are 1.84, 1.36, and 1.54, respectively, in the Mb. 1, Mb. 3, and Mb. 5 (Table 4), indicating that the hydrodynamic force weakens first and then increases from Mb. 1 to Mb. 5.

Moreover, the higher terrestrial inputs only show the higher organic matter content in the Xujiache terrestrial inputs. However, it does not mean that the TOC is higher in the Xujiache sediments, determined by the palaeoproductivity and palaeoenvironment of organic matter [21]. However, terrestrial inputs are correlated to organic matter content in the cross plot (Figures 10(b) and 10(c)). This indicates that the terrestrial inputs are the main controlling

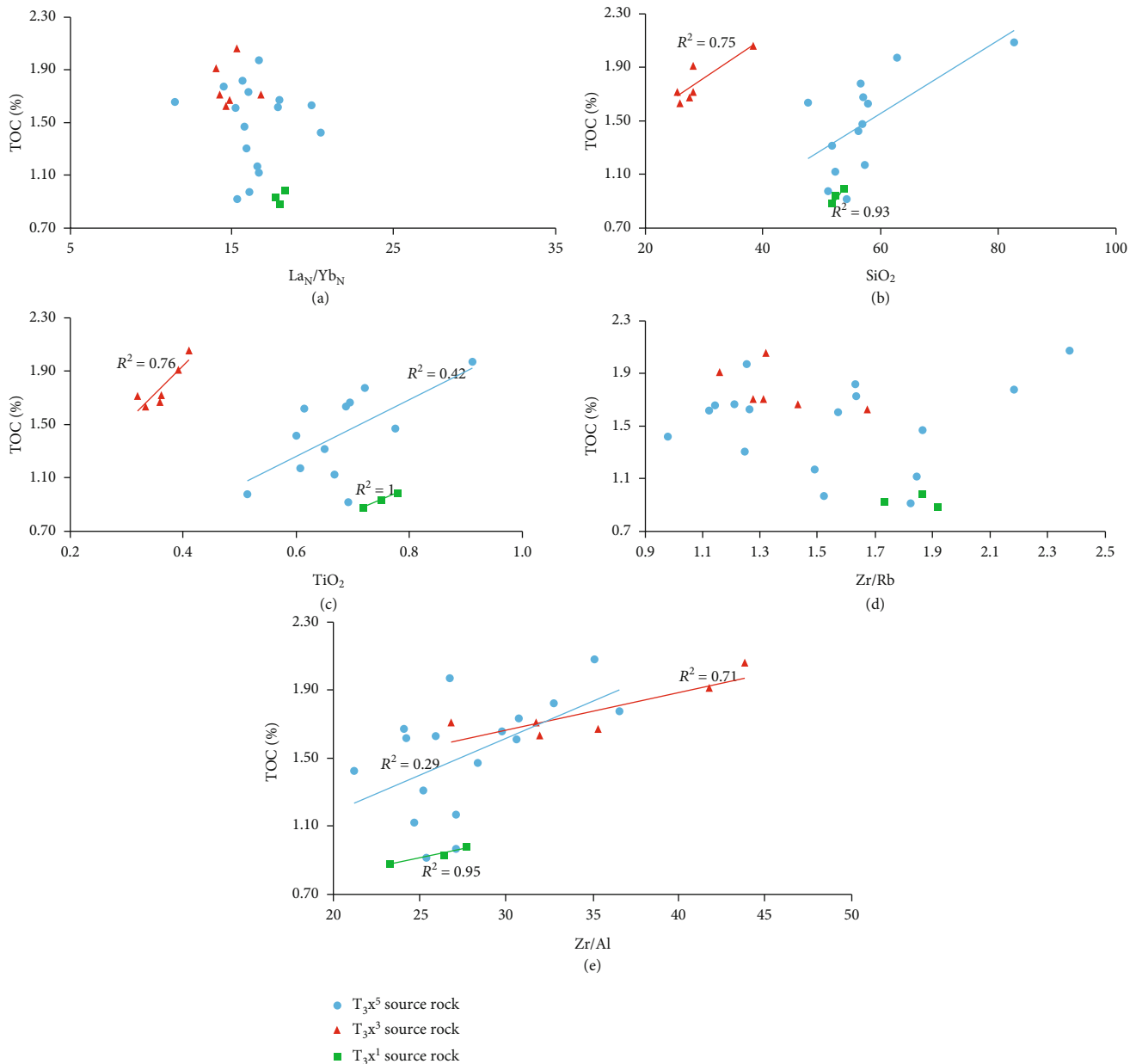


FIGURE 10: Cross plot of TOC with (a) weathering degree, (b, c) terrestrial inputs, (d) hydrodynamics, and (e) sedimentation rate. TOC is positively correlated with terrestrial inputs and sedimentation rate, but not with weathering degree and hydrodynamics.

factor affecting organic matter enrichment in the Xujiahe coal-bearing source rocks. However, no correlation between hydrodynamic parameters and TOC indicates that hydrodynamic conditions are not the controlling factor affecting organic matter enrichment in the Xujiahe sediments (Figure 10(d)).

5.2.6. Sedimentation Rate. The sedimentation rate is closely related to organic matter preservation. The fast sedimentation rate is conducive to the rapid deposition and burial of organic matter and the rapid separation from the overlying oxidized water and sedimentary materials, to avoid the oxidation or degradation of the organic matter. In contrast, organic matter is deposited and buried at a very low sedi-

mentation rate, which is not conducive to organic matter preservation owing to the occurrence of much oxidative degradation during the process. Ding et al. [71] proposed that the organic matter enrichment is controlled by the sedimentation rate under oxidation conditions at the sedimentation rate exceeding 10 cm/kyr and determined by the palaeo-productivity and redox at the sedimentation rate low than 10 cm/kyr. It is worth noting that the sedimentation rate proposed by Chen et al. [72] is close to our study area, so it can be used to discuss the sedimentation rate in the study area.

Moreover, the Zr/Al ratio could be regarded as a substitute index of sedimentation rate [73]. The 3rd Mb. sedimentation rate is the highest ($Zr/Al = 35.26$), followed by the

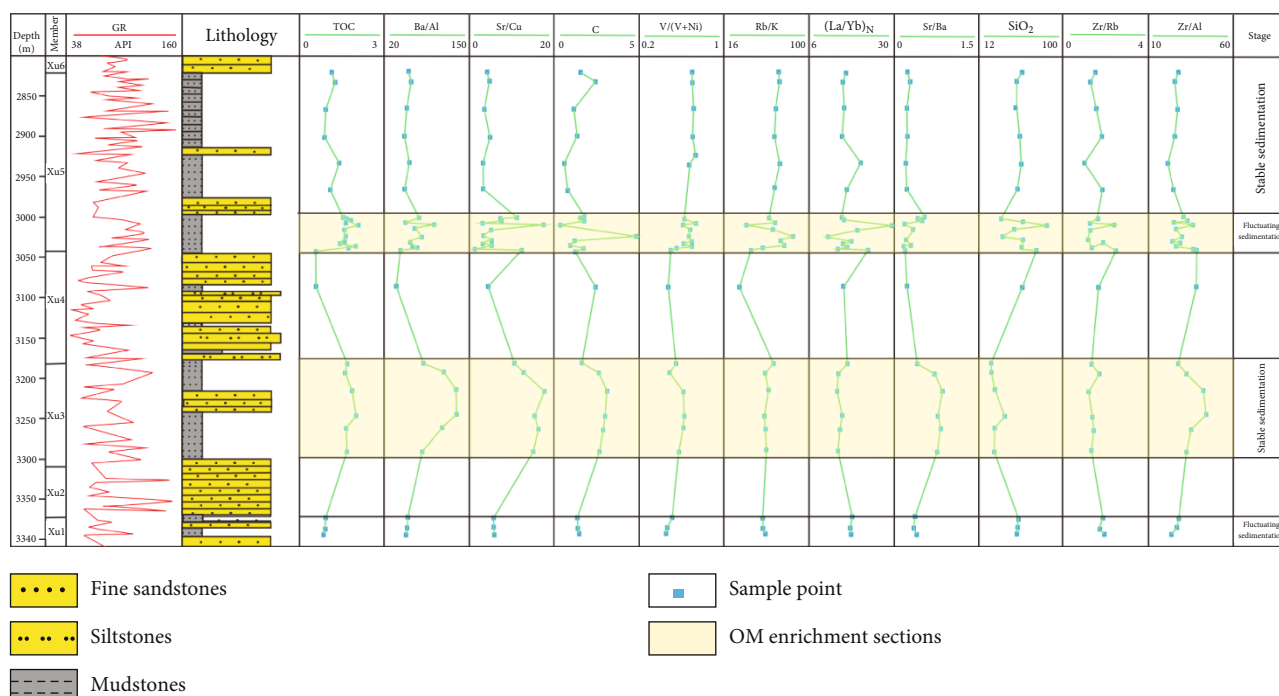


FIGURE 11: Geochemical index profile of Xujiache Formation in well J31, Sichuan Basin.

Mb. 5 ($Zr/Al = 27.96$) (Table 4). The Zr/Al value is the lowest at 25.76 in the Mb. 1. The sedimentation rate is consistent with the index Zr/Al values in the Xujiache sediments. The higher sedimentation rates of Mb. 3 and Mb. 5 are, the more enriched organic matter is. Zr/Al was also positively correlated with TOC (Figure 10(e)). Moreover, the 1st Mb. sedimentation rate less than 10 cm/kyr should be controlled by palaeoproductivity and redox. However, it has a good correlation with the sedimentation rate, which is contrary to the result done by Ding et al. [71] (Figure 10(e)). This may be related to the threshold values of sedimentation rate in different basins. In short, it can be deduced that sedimentation rate is the main controlling factor affecting organic matter enrichment in the Xujiache coal-bearing source rocks.

5.3. Evolution of the Palaeoenvironment

5.3.1. Xujiache Palaeosedimentary Environment. The Xujiache palaeoenvironment was characterized by a humid to arid climate, oxygen-rich, fresh-brackish water environment, shallow water depth, moderate terrestrial inputs, hydrodynamic and weathering conditions, and high sedimentation rates. Moreover, the Xujiache climate was warm and humid in the Sichuan Basin (Figure 11). However, there was a hot climate interval during a short geological period (Figure 11). This supports the view that the global climate is complex in the Late Triassic. The water in the Sichuan Basin was rich in oxygen during the Xujiache period, indicating that the global Late Triassic anoxic event did not spread to continental lake basins.

Additionally, the sedimentary environment of Xujiache source rocks has been analyzed by many scholars. The Mb.

1 was formed in a transitional period, which was featured with normal marine pelecypod fossils, marine tidal reverse cross-bedding and cross-laminae [74]. Moreover, the 1st Mb. source rocks have a thin thickness owing to the tectonic frequent changes in the sedimentary period. The 3rd Mb. source rocks are developed in the stable stage of transitional facies with a certain thickness and large distributed area because of the relatively stable structure in which marine sedimentary structures, glauconite, and brackish Lamelli-branchiata fossils were found [74–76]. The previous scholars suggested that the 5th Mb. source rocks with large thickness are developed in the continental sedimentary facies owing to the relatively stable structure [37]. However, Zhao and Zhang [74] and Shi et al. [41] believed that the Mb. 5 is characterized by transitional sediments because of the occurrence of marine sedimentary structures and high salinity. However, this viewpoint is debatable because the limited samples of 5th Mb. source rocks taken by these scholars are not sufficient to evaluate the overall 5th Mb. sedimentary characteristics. However, it can be deduced that the Mb. 5 has marine sedimentary characteristics, which may be caused by the unstable structural activity during the Mb. 4 to Mb. 5 sedimentary transitional periods [77].

According to the longitudinal variation of geochemical parameters and the previous study of sedimentary characteristics (Figure 11), the Xujiache sedimentary environment can be divided into four sedimentary stages: (1) fluctuating stage of transitional sedimentation (FSTS) (Mb. 1) (3370 m–3405 m): the high salinity, shallow water depth, low sedimentation rate, and strong hydrodynamic force; (2) stable stage of transitional sedimentation (SSTS) (Mb. 3) (3000 m–3050 m): the highest salinity, hot weather, appropriate water depth, weak hydrodynamic force, and high

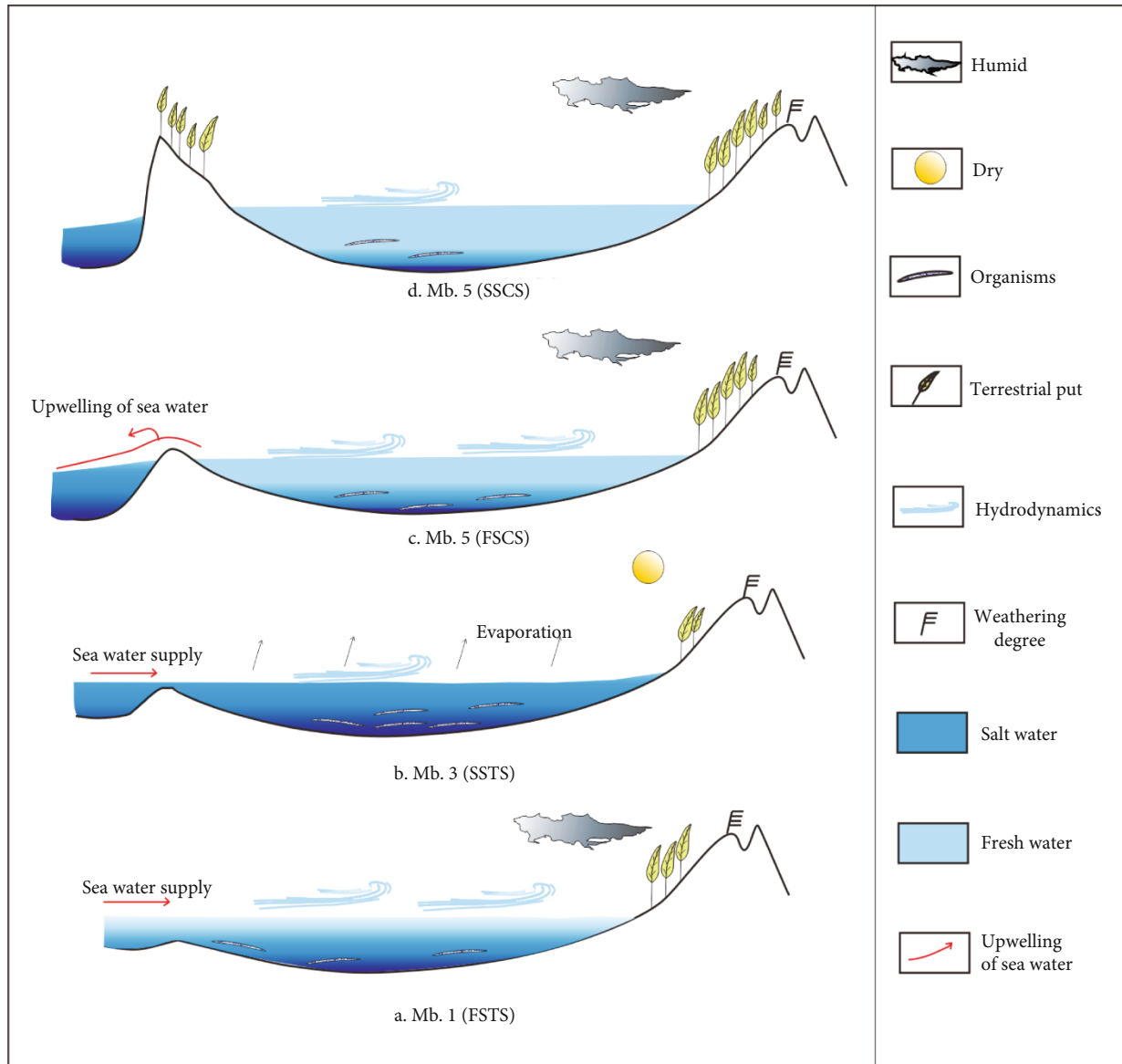


FIGURE 12: Sedimentary environment evolution model of Xujiahe Formation, Sichuan Basin.

deposition rate; (3) fluctuating stage of continental sedimentation (FSCS) (Mb. 5) (3180 m-3310 m): the transgressions and terrestrial inputs resulting in frequent changes in the water salinity, water depth, degree of oxidation, terrestrial inputs, and hydrodynamics because of the unstable Longmenshan tectonic movement and unclosed estuary; (4) stable stage of continental sedimentation (SSCS) (Mb. 5) (2820 m-3000 m). The further uplifted Longmenshan structure leads that the Xujiahe Formation completely entered the continental sedimentation with the water salinity significantly reduced, the water depth deepened, and the terrestrial inputs increased.

5.3.2. Sedimentary Evolution. The sedimentary evolution is determined in different Xujiahe sedimentary periods according to the analysis of the Xujiahe sedimentary environment and geological background.

The climate was humid, and the water was shallow with high salinity and strong hydrodynamics and high oxidation and connected to the PTC during the 1st Mb. sedimentary period (Figure 12(a)). Moreover, the strong weathering led to more terrestrial inputs. The terrestrial inputs increased during the 1st Mb. sedimentary period because the Centre Sichuan area was far away from the estuary with a thinner source rock and higher terrestrial inputs [37]. In contrast, the closer the source rocks were to the estuary of the Longmenshan, the higher the reducibility and salinity of the water, and the lower the terrestrial inputs [78].

Some areas were connected to the PTC in the 3rd Mb. sedimentary period because the northern part of Longmenshan was uplifted [30]. The climate of the 3rd Mb. was slightly hot and dry comparable with the 1st Mb. sedimentary period, leading to the increase of the water depth, reducibility

and salinity, and the reduction of the hydrodynamic force, weathering, and terrestrial inputs (Figure 12(b)).

The PTC was not connected to the lake in the Sichuan Basin owing to the uplift of the Longmenshan [79]. Compared with the 3rd Mb. sedimentary period, the climate was humid with the increased water depth and reducibility and the decreased water salinity in the Mb. 5. Moreover, the hydrodynamics, weathering, and terrestrial inputs increased. The Mb. 5 was characterized by two sedimentation stages, including FSCS and SSCS. Compared with the SSCS, the water has higher salinity and deposition rate in the FSCS (Figures 12(c) and 12(d)).

5.4. Connection between Xujiahe Source Rocks with the PTC. The 1st and 3rd Mbs. sedimentary periods were characterized by the high water salinity, high palaeoproductivity, abundant dinosteranes, low Pr/Ph ratios, and high low carbon number n-alkanes according to the analysis in Sections 5.1 and 5.2 (Tables 1 and 4; Figures 2–4). Low Pr/Ph ratios and high low carbon number n-alkanes are very rare in the terrestrial source rocks, indicating that they are affected by transgression (Table 1; Figure 3). The dinosterane is a biomarker in the marine environment [45, 80, 81]. These organic and inorganic geochemical indicators all prove that the water was connected with the PTC in the 1st and 3rd Mbs. period.

Additionally, the source rocks had high TOC content, palaeoproductivity, and dinosteranes and lower Pr/Ph values in the FSCS (Tables 1 and 4). Furthermore, abundant algae and dinosteranes were found under fluorescence (Figures 2 and 4). This indicates that the PTC was still connected with the water of Mb. 5 in the FSCS. Although the Longmenshan was uplifted, the Late Triassic giant monsoon environment led to the intermittent connection between the PTC and water of Mb. 5 in the FSCS [82]. However, the TOC content decreased with the decreased palaeoproductivity, undeveloped dinosteranes, low algal substance, and higher Pr/Ph ratios in the SSCS (Tables 1 and 4; Figures 2 and 4). This indicated that the PTC was completely disconnected with the water of Mb. 5 at the end of the FSCS owing to the further uplift of the Longmenshan.

5.5. Dynamic Formation Mechanism of the Organic Matter. Although the water of Mb. 1 was connected with the PTC in the FSTS, the shallow water depth, strong hydrodynamic force, and low sedimentation rate were not conducive to the organic matter preservation. The Mb. 3 was still connected with the PTC in the SSTS, which brought abundant marine organic matter to the Xujiahe water. Moreover, the weak hydrodynamic force and high deposition rate were conducive to the large organic matter accumulation. The continental sedimentation showed distinctive characteristics. One period was characterized by high Ba/Al, Sr/Cu, Zr/Rb, and Sr/Ba and low SiO₂ in the FSCS (Figure 11). This suggested a connection between the lake basin and the PTC during the 5th Mb. sedimentary period. Moreover, the intermittent transgression increased the salinity of the Xujiahe water and brought abundant marine organisms, facilitating the temporary development of organisms. The other period was characterized by high Ba/Al, SiO₂, and Zr/Rb and low

Rb/K and Sr/Ba in the FSCS (Figure 11). This showed that terrestrial inputs brought abundant terrestrial organisms and increased biological productivity in a sedimentary period. Moreover, the structure and palaeoproductivity tended to be stable in the SSCS. The organic matter was derived from terrestrial inputs, resulting in decreased biological productivity.

The TOC was positively correlated with the biological productivity, terrestrial inputs, and sedimentation rate in the Xujiahe sediment according to Section 5.2. Climate, water depth, redox, salinity, weathering, and hydrodynamics were not the main factors for organic matter enrichment in the Xujiahe sedimentary period. The dynamic mechanism of the organic matter enrichment (input-rapid subsidence model) was established according to the Xujiahe palaeoenvironment (Figure 13).

The weak orogeny led to a stable sedimentary environment in the 1st, 3rd, and 5th Mbs. deposition, which supports the conditions for the development of source rocks. A stable environment was favorable for the organic matter enrichment. Moreover, abundant marine organic matter led to an increase in the organic matter content in the Xujiahe Formation owing to the connection between the Xujiahe water with the PTC. Strong terrestrial inputs and high sedimentation rate also reduced the oxidation and decomposition of the organic matter, which was beneficial to its preservation, thereby resulting in the formation of the source rocks.

5.6. High-Quality Coal-Bearing Source Rocks. The evaluation of source rocks mainly includes the organic matter abundance, kerogen type, and maturity. The organic matter abundance is mainly used to present the organic matter content, and the relationship between TOC and S₁+S₂ is generally used to represent the organic matter content in source rocks. According to the evaluation criteria of coal-bearing source rocks [83], Figure 14 shows that the good source rocks are well developed in the SSTS and FSCS, which is consistent with the organic matter enrichment sections in Figure 11. The Ro values of the Xujiahe source rocks range from 1.28% to 1.87%, indicating that the source rocks are in the mature to high maturity stage, characterized by producing wet and dry gas.

Coal-bearing source rocks contain more liptinites and exinites, which can produce more oil and gas [84]. The inertinites show black opacity and no fluorescence under transmitted light [85]. The vitrinites are transparent to semi-transparent under transmitted light with a weakly fluorescent rod. The liptinites are transparent under transmitted light with yellow or yellowish-brown colors and strong fluorescence. Table 2 shows that the kerogen types include two types (type II₂ and type III) in the 5th Mb. source rocks. The TI values of type II₂ kerogen range from 1.5 to 27 in the 1st and 3rd Mbs. source rocks. The kerogen is type III in the SSCS with many opaque black inertinites (over 48%) and no fluorescence under a microscope according to the kerogen macerals (Figure 2). In contrast, the kerogen is type II₂ with more liptinites in the FSCS. The kerogen macerals show similar microscopic characteristics under transmitted light and fluorescence in the FSTS, SSTS, and FSCS, wherein

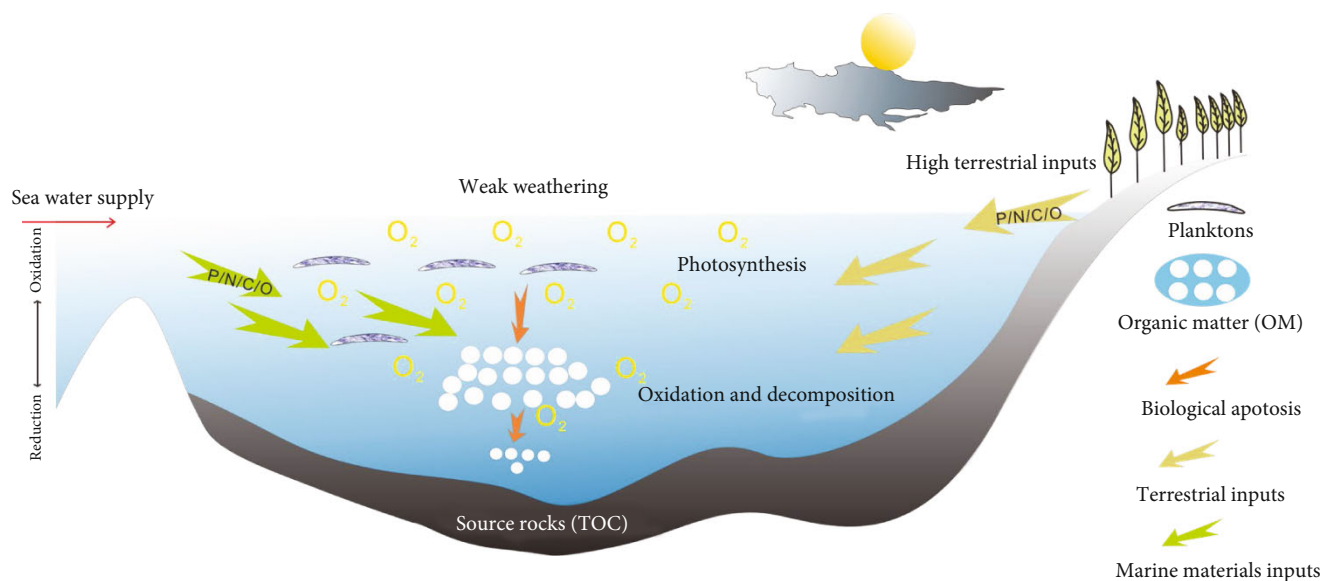


FIGURE 13: Organic matter enrichment mechanism in the Xujiahe Formation, Sichuan Basin. A certain connection with the PTC led to the increase of the Xujiahe organic matter content. Terrestrial organic matter inputs also contributed to the organic matter enrichment. The strong terrestrial inputs and sedimentation rate reduced the oxidation and decomposition of the organic matter and benefited the organic matter preservation.

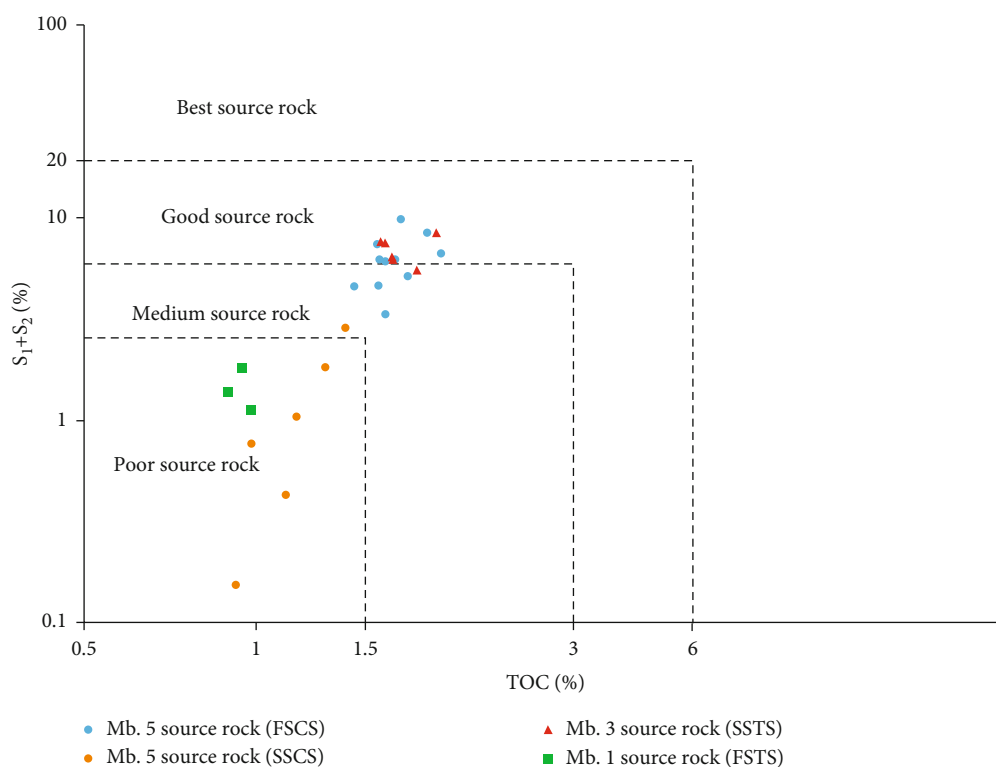


FIGURE 14: Cross plot of TOC with S_1+S_2 of Xujiahe Formation, Sichuan Basin.

many amorphous and transparent liptinites exist (Figure 2). However, many studies have reported that the kerogen of the Xujiahe source rocks is type III in the Sichuan Basin [86, 87]. In contrast, the OM in the study area is characterized by type II₂ kerogen, which produces more oil and gas [84].

The Xujiahe source rocks are comprehensively evaluated as the high-quality coal-bearing source rocks in the SSTS and FSCS with the high TOC and maturity, and good parent material, which can produce large amounts of gas. The formation of high-quality coal-bearing source rocks is closely

related to the connection of the PTC and Xujiache water, the terrestrial inputs, and the sedimentation rate.

6. Conclusions

The climate of the Xujiache Formation was generally warm and humid in the Sichuan Basin, whereas a hot climate existed for a short geological period. This supports the view that the global Late Triassic climate is complex. The global ocean anoxic climate did not spread to the continental lake basin in the Late Triassic. The Palaeo-Tethys Ocean withdrew westward from the Yangtze plate in the late period of the fluctuating stage of continental sedimentation.

- (1) The Xujiache sedimentary environment can be divided into a fluctuating stage of transitional sedimentation, stable stage of transitional sedimentation, fluctuating stage of continental sedimentation, and stable stage of continental sedimentation. The Xujiache water was connected with the Palaeo-Tethys Ocean in the stable and fluctuating stages of transitional sedimentation. The Xujiache sediments were influenced by multiple intermittent transgression and terrestrial inputs owing to the incomplete withdrawal of the PTC and tectonic fluctuation in the fluctuating stage of continental sedimentation. The Xujiache water was not connected with the Palaeo-Tethys Ocean because of the continuous tectonic uplift in the stable stage of continental sedimentation
- (2) The source rocks with type II₂ kerogen have abundant algae and dinosteranes and low Pr/Ph ratios owing to the connection with the Palaeo-Tethys Ocean in the stable and fluctuating stages of transitional sedimentation and fluctuating stage of continental sedimentation. The presence of these materials is closely related to the inputs of marine materials. However, the water was not connected with the Palaeo-Tethys Ocean in the stable stage of continental sedimentation, leading to no algae in the source rocks with type III kerogen
- (3) The Xujiache source rocks are high-quality coal-bearing source rocks in the stable stage of transitional sedimentation and fluctuating stage of continental sedimentation with high total organic carbon and maturity and good parent material. The abundant marine organic matter increased the Xujiache organic matter content. The strong terrestrial inputs and high sedimentation rate simultaneously increased the organic matter deposition and reduced the oxidative decomposition of organic matter, which was beneficial to the organic matter preservation

Data Availability

The data that support the findings of this study are available on request from the corresponding author. The data are not publicly available due to privacy restrictions.

Conflicts of Interest

We declare that we have no financial and personal relationships with other people or organizations that can inappropriately influence our work, and there is no professional or other personal interest of any nature or kind in any product, service, and/or company that could be construed as influencing the position presented in, or the review of, the manuscript entitled “Palaeosedimentary Environment and Formation Mechanism of High-Quality Xujiache Source Rocks, Sichuan Basin, South China.”

Authors' Contributions

Kun Xu wrote and prepared the original draft and contributed to the software and experiment. Shijia Chen performed the conceptualization. Jungang Lu contributed to the data processing and data curation methodology. Yong Li performed the investigation. Xingcheng Zhu helped in the software and validation. Jihua Liu wrote, reviewed, and edited the manuscript. Xueting Wu performed the experiment and software. Chen Li contributed to the data processing.

Acknowledgments

This study was supported by the Natural Science Foundation of China (41872165), the Science and Technology Cooperation Project of the CNPC-SWPU Innovation Alliance (2020CX030000 and 2020CX050000), and the Research and Innovation Fund of Southwest Petroleum University (2021CXYB57).

References

- [1] Y. C. Liu, D. X. Chen, N. S. Qiu, J. Fu, and J. K. Jia, “Geochemistry and origin of continental natural gas in the western Sichuan basin, China,” *Journal of Natural Gas Science and Engineering*, vol. 49, pp. 123–131, 2018.
- [2] J. X. Dai, Y. Y. Ni, Q. Y. Liu et al., “Sichuan super gas basin in southwest China,” *Petroleum Exploration and Development*, vol. 48, no. 6, pp. 1251–1259, 2021.
- [3] H. W. Tipper, E. S. Carter, M. J. Orchard, and E. T. Tozer, “La limite Trias-Jurassique dans les îles de la Reine Charlotte en Colombie-Britannique définie par les ammonites, conodontes et les radiolaires,” *Geobios*, vol. 27, pp. 485–492, 1994.
- [4] J. C. Crowell, “Pre-Mesozoic ice ages: their bearing on understanding the climate system,” *Memoir of the Geological Society of America*, vol. 192, pp. 1–112, 1992.
- [5] N. Tian, Y. Wang, M. Philippe, L. Li, X. Xie, and Z. Jiang, “New record of fossil wood *Xenoxylon* from the Late Triassic in the Sichuan Basin, southern China and its paleoclimatic implications,” *Palaeogeography, Palaeoclimatology, Palaeoecology*, vol. 464, pp. 65–75, 2016.
- [6] L. H. Tanner, J. F. Hubert, B. P. Coffey, and D. P. McInerney, “Stability of atmospheric CO₂ levels across the Triassic/Jurassic boundary,” *Nature*, vol. 411, no. 6838, pp. 675–677, 2001.
- [7] P. A. Hochuli and J. O. Vigran, “Climate variations in the Boreal Triassic – inferred from palynological records from the Barents Sea,” *Palaeogeography Palaeoclimatology Palaeoecology*, vol. 290, no. 1–4, pp. 20–42, 2010.

- [8] L. Q. Li and Y. D. Wang, "Late Triassic palynofloras in the Sichuan Basin, South China: synthesis and perspective," *Palaeoworld*, vol. 25, no. 2, pp. 212–238, 2016.
- [9] L. Q. Li, Y. D. Wang, Z. S. Liu, N. Zhou, and Y. Wang, "Late Triassic palaeoclimate and palaeoecosystem variations inferred by palynological record in the northeastern Sichuan Basin, China," *Palontologische Zeitschrift*, vol. 90, no. 2, pp. 327–348, 2016.
- [10] M. Barbacka, G. Pacyna, Á. T. Kocsis, A. Jarzynka, J. Ziája, and E. Bodor, "Changes in terrestrial floras at the Triassic-Jurassic boundary in Europe," *Palaeogeography Palaeoclimatology Palaeoecology*, vol. 480, pp. 80–93, 2017.
- [11] J. H. Whiteside, P. E. Olsen, D. V. Kent, S. J. Fowell, and M. T. Touhami, "Synchrony between the Central Atlantic magmatic province and the Triassic-Jurassic mass-extinction event?," *Palaeogeography Palaeoclimatology Palaeoecology*, vol. 244, no. 1–4, pp. 345–367, 2007.
- [12] M. Hautmann, F. Stiller, H. W. Cai, and J. G. Sha, "Extinction-recovery pattern of level-bottom faunas across the Triassic-Jurassic boundary in Tibet: implications for potential killing mechanisms," *PALAIOS*, vol. 23, no. 10, pp. 711–718, 2008.
- [13] A. M. C. Sengör, "Mid-Mesozoic closure of Permo-Triassic Tethys and its implications," *Nature*, vol. 279, no. 5714, pp. 590–593, 1979.
- [14] J. W. Zi, P. A. Cawood, W. M. Fan et al., "Triassic collision in the Paleo-Tethys Ocean constrained by volcanic activity in SW China," *Lithos*, vol. 144–145, pp. 145–160, 2012.
- [15] I. Metcalfe, "Gondwana dispersion and Asian accretion: tectonic and palaeogeographic evolution of eastern Tethys," *Journal of Asian Earth Sciences*, vol. 66, pp. 1–33, 2013.
- [16] H. J. Song, J. N. Tong, Y. L. Xiong, D. Y. Sun, L. Tian, and H. Y. Song, "The large increase of $\delta^{13}\text{C}_{\text{carb}}$ -depth gradient and the end-Permian mass extinction," *Science China Earth Sciences*, vol. 55, no. 7, pp. 1101–1109, 2012.
- [17] Y. J. Wang, X. Qian, P. A. Cawood et al., "Closure of the East Paleotethyan Ocean and amalgamation of the Eastern Cimmerian and Southeast Asia continental fragments," *Earth-Science Reviews*, vol. 186, pp. 195–230, 2018.
- [18] Y. Zheng, H. B. Li, H. Wang, H. Zhang, and C. L. Li, "Indosinian thrust—nappe structure and its sedimentary response in the Longmen Mts. Thrust Belt," *Geological Review*, vol. 64, no. 1, pp. 45–61, 2018.
- [19] M. Pole, Y. D. Wang, C. Dong et al., "Fires and storms—a Triassic-Jurassic transition section in the Sichuan Basin, China," *Palaeobiodiversity & Palaeoenvironments*, vol. 98, no. 1, pp. 29–47, 2018.
- [20] N. Lu, Y. D. Wang, M. E. Popa et al., "Sedimentological and paleoecological aspects of the Norian-Rhaetian transition (Late Triassic) in the Xuanhan area of the Sichuan Basin, southwest China," *Palaeoworld*, vol. 28, no. 3, pp. 334–345, 2019.
- [21] Z. L. Xiao, S. J. Chen, S. M. Zhang et al., "Sedimentary environment and model for lacustrine organic matter enrichment: lacustrine shale of the Early Jurassic Da'anzhai formation, Central Sichuan Basin, China," *Journal of Palaeogeography*, vol. 10, no. 4, pp. 584–601, 2021.
- [22] C. Yan, Z. Jin, J. Zhao, W. Du, and Q. Liu, "Influence of sedimentary environment on organic matter enrichment in shale: a case study of the Wufeng and Longmaxi formations of the Sichuan Basin, China," *Marine and Petroleum Geology*, vol. 92, pp. 880–894, 2018.
- [23] Y. Nie, X. G. Fu, W. L. Xu, H. G. Wen, Z. W. Wang, and C. Y. Song, "Redox conditions and climate control on organic matter accumulation and depletion during the Toarcian in the Qiangtang Basin, eastern Tethys," *International Journal of Earth Sciences*, vol. 109, no. 6, pp. 1977–1990, 2020.
- [24] R. Wakefield, A. D. Woods, T. W. Beatty, and J. P. Zonneveld, "How quickly did primary producers recover from the Permian-Triassic mass extinction? Earliest Triassic (Griesbachian) productivity estimates from the Pedigree-Ring Border-Kahntah River area (Western Canada Sedimentary Basin) northwestern Alberta and northeastern British Columbia," *Geological Society of America*, vol. 42, no. 4, p. 63, 2010.
- [25] I. M. J. Mohialdeen and M. H. Hakimi, "Geochemical characterisation of Tithonian-Berriasian Chia Gara organic-rich rocks in northern Iraq with an emphasis on organic matter enrichment and the relationship to the bioproductivity and anoxia conditions," *Journal of Asian Earth Sciences*, vol. 116, pp. 181–197, 2016.
- [26] W. H. Li, Z. H. Zhang, and Y. C. Li, "Some aspects of excellent marine source rock formation: implications on enrichment regularity of organic matter in continental margin basins," *Chinese Journal of Geochemistry*, vol. 34, no. 1, pp. 47–54, 2015.
- [27] S. Liu, X. G. Ren, S. X. Yao et al., "Relationship between gas reservoir distribution and structural system of upper Triassic Xujiahe Fm in the Sichuan Basin," *Natural Gas Industry B*, vol. 6, no. 3, pp. 220–235, 2019.
- [28] Q. R. Meng, "Origin of the Qinling mountains," *Scientia Sinica Terrae*, vol. 47, no. 4, pp. 412–420, 2017.
- [29] S. F. Liu, R. Steel, and G. W. Zhang, "Mesozoic sedimentary basin development and tectonic implication, northern Yangtze Block, eastern China: record of continent-continent collision," *Journal of Asian Earth Sciences*, vol. 25, no. 1, pp. 9–27, 2005.
- [30] S. F. Liu, T. Qian, W. P. Li, G. X. Dou, and P. Wu, "Oblique closure of the northeastern Paleo-Tethys in central China," *Tectonics*, vol. 34, no. 3, pp. 413–434, 2015.
- [31] X. Tao, "Evolution of nappe tectonic and foreland basin in the southern section of Longmen Mountains," *Journal of the Chengdu Institute of Technology*, vol. 26, no. 1, pp. 73–77, 1999.
- [32] H. Mu, D.-P. Yan, L. Qiu et al., "Formation of the Late Triassic western Sichuan foreland basin of the Qinling Orogenic Belt, SW China: sedimentary and geochronological constraints from the Xujiahe formation," *Journal of Asian Earth Sciences*, vol. 183, article 103938, 2019.
- [33] Z. Qiu and J. L. He, "Depositional environment changes and organic matter accumulation of Pliensbachian-Toarcian lacustrine shales in the Sichuan basin, SW China," *Journal of Asian Earth Sciences*, vol. 232, article 105035, 2022.
- [34] Y. Li, S. J. Chen, W. Qiu, K. M. Su, and B. Y. Wu, "Controlling factors for the accumulation and enrichment of tight sandstone gas in the Xujiahe formation, Guang'an area, Sichuan Basin," *Energy Exploration & Exploitation*, vol. 37, no. 1, pp. 26–43, 2019.
- [35] T. Deng, Y. Li, Z. J. Wang et al., "Geochemical characteristics and organic matter enrichment mechanism of black shale in the Upper Triassic Xujiahe Formation in the Sichuan basin: implications for paleoweathering, provenance and tectonic setting," *Marine and Petroleum Geology*, vol. 109, pp. 698–716, 2019.
- [36] J. Ye, "Assessment of hydrocarbon source rocks in Xu-2 member, Ma'antang Formation, gas system in west Sichuan depression," *Natural Gas Industry*, vol. 23, no. 1, pp. 21–25, 2003.

- [37] W. Z. Zhao, C. S. Qia, C. C. Xu, H. J. Wang, T. S. Wang, and Z. S. Shi, "Assessment on gas accumulation potential and favorable plays within the Xu-1, 3 and 5 members of the Xujiahe formation in the Sichuan Basin," *Petroleum Exploration and Development*, vol. 38, no. 4, pp. 385–393, 2011.
- [38] Z. Y. Gao, B. Bai, R. K. Zhu, L. H. Liu, J. R. Feng, and J. L. Mei, "Reservoir sedimentary response to tectonic movement of the Late Triassic in front of Dabashan and Longmen Mountains," *Journal of Palaeogeography*, vol. 14, no. 6, pp. 802–812, 2012.
- [39] K. Burger, Y. P. Zhou, and Y. L. Ren, "Petrography and geochemistry of tonsteins from the 4th member of the Upper Triassic Xujiahe formation in southern Sichuan Province, China," *International Journal of Coal Geology*, vol. 49, no. 1, pp. 1–17, 2002.
- [40] J. X. Dai, Y. Y. Ni, C. N. Zou et al., "Stable carbon isotopes of alkane gases from the Xujiahe coal measures and implication for gas-source correlation in the Sichuan Basin, SW China," *Organic Geochemistry*, vol. 40, no. 5, pp. 638–646, 2009.
- [41] Z. S. Shi, W. R. Xie, S. Y. Ma, and G. X. Li, "Transgression sedimentary records of the members 4–6 of Upper Triassic Xujiahe Formation in Sichuan Basin," *Journal of Palaeogeography*, vol. 14, no. 5, pp. 583–595, 2012.
- [42] T. G. Powell and D. M. Mokirdy, "The effect of source material, rock type and diagenesis on the n-alkane content of sediments," *Geochimica et Cosmochimica Acta*, vol. 37, no. 3, pp. 623–633, 1973.
- [43] H. L. T. Haven, J. W. D. Leeuw, J. Rullkötter, and J. S. S. Damsté, "Restricted utility of the pristane/phytane ratio as a palaeoenvironmental indicator," *Nature*, vol. 330, no. 6149, pp. 641–643, 1987.
- [44] R. A. Sandaruwan and S. Yoshikazu, "Characterization of organic matter and depositional environment of the Jurassic small sedimentary basins exposed in the northwest onshore area of Sri Lanka," *Researches in Organic Geochemistry*, vol. 31, no. 1, pp. 15–28, 2015.
- [45] D. J. Hou, T. G. Wang, Y. W. Zhang, L. Y. Zhang, and C. L. Zhang, "Dinosteranes in the tertiary terrestrial deposits, eastern china—the marker of marine transgression facies?," *Geological Review*, vol. 43, no. 5, pp. 524–528, 1997.
- [46] N. B. Harris, K. H. Freeman, R. D. Pancost, T. S. White, and G. D. Mitchell, "The character and origin of lacustrine source rocks in the lower cretaceous synrift section, Congo Basin, West Africa," *AAPG Bulletin*, vol. 88, no. 8, pp. 1164–1184, 2004.
- [47] D. T. Yan, D. Z. Chen, Z. Z. Wang, J. Li, X. R. Yang, and B. Zhang, "Climatic and oceanic controlled deposition of Late Ordovician-Early Silurian black shales on the North Yangtze platform, South China," *Marine and Petroleum Geology*, vol. 110, pp. 112–121, 2019.
- [48] C. Liang, Z. X. Jiang, Y. C. Cao, J. C. Zhang, and L. Guo, "Sedimentary characteristics and paleoenvironment of shale in the Wufeng-Longmaxi Formation, North Guizhou Province, and its shale gas potential," *Journal of Earth Science*, vol. 28, no. 6, pp. 1020–1031, 2017.
- [49] A. Reitz, K. Pfeifer, G. J. D. Lange, and J. Klump, "Biogenic barium and the detrital Ba/Al ratio: a comparison of their direct and indirect determination," *Marine Geology*, vol. 204, no. 3–4, pp. 289–300, 2004.
- [50] J. K. Mckay and T. F. Pedersen, "The accumulation of silver in marine sediments: a link to biogenic Ba and marine productivity," *Global Biogeochemical Cycles*, vol. 22, no. 4, pp. 1–17, 2008.
- [51] J. Dymond, E. Suess, and M. Lyle, "Barium in deep-sea sediment: a geochemical proxy for paleoproductivity," *Paleoceanography*, vol. 7, no. 2, pp. 163–181, 1992.
- [52] W. J. Bonn, F. X. Gingele, H. Grobe, A. Mackensen, and D. K. Futterer, "Palaeoproductivity at the Antarctic continental margin: opal and barium records for the last 400 ka," *Palaeogeography, Palaeoclimatology, Palaeoecology*, vol. 139, no. 3–4, pp. 195–211, 1998.
- [53] T. J. Algeo, K. Kuwahara, H. Sano et al., "Spatial variation in sediment fluxes, redox conditions, and productivity in the Permian-Triassic Panthalassic Ocean," *Palaeogeography Palaeoclimatology Palaeoecology*, vol. 308, no. 1–2, pp. 65–83, 2011.
- [54] R. W. Murray and M. Leinen, "Chemical transport to the sea-floor of the equatorial Pacific Ocean across a latitudinal transect at 135°W: tracking sedimentary major, trace, and rare earth element fluxes at the Equator and the Intertropical Convergence Zone," *Geochimica et Cosmochimica Acta*, vol. 57, no. 17, pp. 4141–4163, 1993.
- [55] Y. H. Chen, Y. B. Wang, M. Q. Guo et al., "Differential enrichment mechanism of organic matters in the marine-continental transitional shale in northeastern Ordos Basin, China: control of sedimentary environments," *Journal of Natural Gas Science and Engineering*, vol. 83, article 103625, 2020.
- [56] Z. Y. Zhao, J. H. Zhao, H. J. Wang, J. D. Liao, and C. M. Liu, "Distribution characteristics and applications of trace elements in Junggar basin," *Natural Gas Exploration and Development*, vol. 30, no. 2, pp. 30–40, 2007.
- [57] J. L. Jia, Z. J. Liu, A. Bechtel, S. A. I. Strobl, and P. C. Sun, "Tectonic and climate control of oil shale deposition in the Upper Cretaceous Qingshankou Formation (Songliao Basin, NE China)," *International Journal of Earth Sciences*, vol. 102, no. 6, pp. 1717–1734, 2013.
- [58] T. J. Algeo and J. B. Maynard, "Trace-element behavior and redox facies in core shales of Upper Pennsylvanian Kansas-type cyclothems," *Chemical Geology*, vol. 206, no. 3–4, pp. 289–318, 2004.
- [59] J. R. Hatch and J. S. Leventhal, "Relationship between inferred redox potential of the depositional environment and geochemistry of the Upper Pennsylvanian (Missourian) Stark Shale Member of the Dennis Limestone, Wabaunsee County, Kansas, U.S.A.," *Chemical Geology*, vol. 99, no. 1–3, pp. 65–82, 1992.
- [60] M. A. Arthur and B. B. Sageman, "Marine black shales: depositional mechanisms and environments of ancient deposits," *Annual Review of Earth & Planetary Sciences*, vol. 22, no. 1, pp. 499–551, 1994.
- [61] W. Wei and J. A. Thomas, "Secular variation in the elemental composition of marine shales since 840 Ma: tectonic and seawater influences," *Geochimica et Cosmochimica Acta*, vol. 287, pp. 367–390, 2020.
- [62] A. H. Wang, "Discriminant effect of sedimentary environment by the Sr/Ba ratio of different existing forms," *Acta Sedimentologica Sinica*, vol. 3, no. 2, pp. 297–304, 1996.
- [63] X. G. Zhang, C. Y. Lin, M. A. Zahid, X. P. Jia, and T. Zhang, "Paleosalinity and water body type of Eocene Pinghu Formation, Xihu Depression, East China Sea Basin," *Journal of Petroleum Science and Engineering*, vol. 158, pp. 469–478, 2017.
- [64] W. Yang, R. Zuo, D. X. Chen et al., "Climate and tectonic-driven deposition of sandwiched continental shale units: new insights from petrology, geochemistry, and integrated provenance analyses (the western Sichuan subsiding Basin,

- Southwest China),” *International Journal of Coal Geology*, vol. 211, article 103227, 2019.
- [65] Z. H. Xu, Z. C. Wang, S. Y. Hu, S. F. Zhu, and Q. C. Jiang, “Paleoclimate during depositional period of the Upper Triassic Xujiahe Formation in Sichuan Basin,” *Journal of Palaeogeography*, vol. 12, no. 4, pp. 415–424, 2010.
- [66] J. F. Feng, K. T. Milkeviciene, and J. F. Sarg, “Source rock characteristics in the Green River Oil Shale, Piceance Creek Basin, Colorado—an integrated geochemical and stratigraphic analysis,” in *AAPG Annual Conference and Exhibition*, Houston, Texas, USA, 2011.
- [67] S. K. Hong, K. B. Lee, H. S. Lee, J. Y. Choi, and A. Mort, “Assessment of shale gas potential from geochemical data in the Late Devonian shale succession, Liard Basin, Canada,” *Journal of Petroleum Science and Engineering*, vol. 199, article 108273, 2021.
- [68] L. Tang, Y. Song, X. Q. Pang et al., “Effects of paleo sedimentary environment in saline lacustrine basin on organic matter accumulation and preservation: a case study from the Dongpu Depression, Bohai Bay Basin, China,” *Journal of Petroleum Science and Engineering*, vol. 185, no. 3, article 106669, 2020.
- [69] Q. L. Xu, B. Liu, Y. S. Ma et al., “Controlling factors and dynamical formation models of lacustrine organic matter accumulation for the Jurassic Da’anzhai Member in the central Sichuan Basin, southwestern China,” *Marine and Petroleum Geology*, vol. 86, pp. 1391–1405, 2017.
- [70] H. Dypvik and N. B. Harris, “Geochemical facies analysis of fine-grained siliciclastics using Th/U, Zr/Rb and (Zr+Rb)/Sr ratios,” *Chemical Geology*, vol. 181, no. 1–4, pp. 131–146, 2001.
- [71] X. J. Ding, G. D. Liu, M. Zha et al., “Relationship between total organic carbon content and sedimentation rate in ancient lacustrine sediments, a case study of Erlian basin, northern China,” *Journal of Geochemical Exploration*, vol. 149, pp. 22–29, 2015.
- [72] B. Chen, Y. Li, T. Deng, S. Dong, and W. Hu, “The sedimentary environment and organic matter enrichment pattern of Xujiahe formation shale in the Late Triassic Longmenshan foreland basin, SW China,” *Scientia Geologica Sinica*, vol. 54, no. 2, pp. 434–451, 2019.
- [73] T. Deng, *Black shales characteristics and organic matter enrichment mechanism of Xujiahe formation in the southwestern LongmenShan Foreland Basin*, [Ph.D thesis], Chengdu University of Technology, 2020.
- [74] X. F. Zhao and W. L. Zhang, “A re-discussion on the origins of tidal deposits in the Xujiahe Formation of the Sichuan Basin: further evidences and sequence analysis,” *Natural Gas Industry*, vol. 31, no. 9, pp. 25–30, 2011.
- [75] Q. H. Luo, “Discovery of water-transgression cause filling sands-bodies in ancient sediments- an approach to the genesis of certain upper Triassic sand-bodies in the middle-western part of the Sichuan Basin and discussion on water-transgression delta,” *Acta Sedimentologica Sinica*, vol. 1, no. 3, pp. 59–68, 1983.
- [76] X. F. Zhao, Z. G. Lv, W. L. Zhang, H. R. Peng, and R. D. Kang, “Paralic tidal deposits in the upper Triassic Xujiahe formation in Anyue area, the Sichuan basin,” *Natural Gas Industry*, vol. 28, no. 4, pp. 14–18, 2008.
- [77] L. Yang and L. Z. Deng, “High resolution sequence stratigraphy analysis of xu4 ~ 5 members of Huanglongchang-Dukouhe structure in northeast Sichuan,” *Journal of Oil and Gas Technology*, vol. 30, no. 1, pp. 188–191, 2008.
- [78] X. P. Xie, S. Z. Li, N. Lu, Y. D. Wang, and S. N. Xi, “Sedimentary facies and environment evolution of the 1st member of the Xujiahe formation in Guangyuan area, northern Sichuan,” *Acta Sedimentologica Sinica*, vol. 39, no. 2, pp. 494–505, 2021.
- [79] Q. H. Luo, “Significance of the Anxian movement to the stratigraphic division and correlation of the Upper Triassic formations and their hydrocarbon exploration in the western-central Sichuan Basin,” *Natural Gas Industry*, vol. 31, no. 6, pp. 21–27, 2011.
- [80] M. A. McCaffrey, J. M. Moldowan, P. A. Lipton et al., “Paleoenvironmental implications of novel C₃₀ steranes in Precambrian to Cenozoic Age petroleum and bitumen,” *Geochimica et Cosmochimica Acta*, vol. 58, no. 1, pp. 529–532, 1994.
- [81] N. S. Goodwin, A. L. Mann, and R. L. Patience, “Structure and significance of C₃₀ 4-methyl steranes in lacustrine shales and oils,” *Organic Geochemistry*, vol. 12, no. 5, pp. 495–506, 1988.
- [82] J. Golonka, M. I. Ross, and C. R. Scotese, “Phanerozoic paleogeographic and paleoclimatic modeling maps,” *Pangea: Global Environments and Resources*, vol. 17, pp. 1–47, 1994.
- [83] J. P. Chen, C. Y. Zhao, and Z. H. He, “Criteria for evaluating the hydrocarbon generating potential of organic matter in coal measures,” *Petroleum Exploration and Development*, vol. 24, no. 1, pp. 1–5, 1997.
- [84] B. Tissot, B. Durand, J. Espitalie, and A. Combaz, “Influence of nature and diagenesis of organic matter in formation of petroleum,” *AAPG Bulletin*, vol. 58, no. 3, pp. 499–506, 1974.
- [85] J. Q. Tu, S. Z. Wang, and X. D. Fei, “Classification of the macerals of kerogen in hydrocarbon source rocks by transmitted light fluorescence,” *Petroleum Exploration and Development*, vol. 25, no. 2, pp. 27–29, 1998.
- [86] Y. Yang, S. Y. Wang, L. Huang, and J. G. Zhong, “Features of source rocks in the Xujiahe formation at the transitional zone of central-southern Sichuan Basin,” *Natural Gas Industry*, vol. 29, no. 6, 2009.
- [87] J. X. Dai, Y. Y. Ni, and C. N. Zou, “Stable carbon and hydrogen isotopes of natural gases sourced from the Xujiahe formation in the Sichuan Basin, China,” *Organic Geochemistry*, vol. 43, no. 2, pp. 103–111, 2012.
- [88] K. H. Wedepohl, “Environmental influences on the chemical composition of shales and clays,” *Physics & Chemistry of the Earth*, vol. 8, pp. 307–333, 1971.
- [89] K. H. Wedepohl, “The composition of the upper Earth’s crust and the natural cycles of selected elements. Metals in natural raw materials, natural resources,” *Metals and Their Compounds in the Environment. Occurrence, Analysis and Biological Relevance*, pp. 3–17, 1991.